Electronic Supplementary Information

Synthesis and electron-transport property of stable antiaromatic Ni^{II} norcorrole with the smallest *meso*-substituent

Shusaku Ukai,[a] Yun Hee Koo,[a] Norihito Fukui,[a] Shu Seki,*[b] and Hiroshi Shinokubo*[a]

[a]Department of Molecular and Macromolecular Chemistry, Graduate School of Engineering, Nagoya University, Furo-cho, Chikusa-ku, Nagoya 464-8603, Japan.
[b]Department of Molecular Engineering, Graduate School of Engineering, Kyoto University, Nishikyo-ku, Kyoto 615-8510, Japan

E-mail: hshino@chembio.nagoya-u.ac.jp; seki@moleng.kyoto-u.ac.jp

1. Instrumentation and Materials

^{1}H NMR (500 MHz) and ^{13}C NMR (126 MHz) spectra were recorded on a Varian INOVA-500 spectrometer. Chemical shifts were reported as the delta scale in ppm relative to $CHCl_3$ ($\delta = 7.260$ ppm) for ^{1}H NMR and $CDCl_3$ ($\delta = 77.0$ ppm) for ^{13}C NMR. UV/vis/NIR absorption spectra were recorded on a Shimadzu UV-2550 or JASCO V670 spectrometer. High-resolution electrospray ionization time-of-flight (ESI-TOF) mass spectra were taken on Bruker microTOF instrument. Matrix assisted laser desorption and ionization time-of-flight mass spectra (MALDI-TOF-MS) were taken on Bruker autoflex max. X-ray data were taken on Rigaku CCD diffractometer (Saturn 724 with MicroMax-007) with Varimax Mo optics using graphite monochromated Mo-Kα radiation (λ = 0.71075 Å). 5-Methyldipyrromethane were synthesized according to the literature.[1] Unless otherwise noted, materials obtained from commercial suppliers were used without further purification.

2. Synthetic Procedures and Compound Data

We previously reported that the reaction of *meso*-phenyldibromodipyrrin Ni^{II} complex **11** with Ni(cod)$_2$ followed by silica-gel chromatography afforded *meso*-diphenylnorcorrole **4** in a low isolated yield of 28% (Scheme S1, method a).[2] To clarify the reason for this low yield, we subjected *meso*-mesityldibromodipyrrin Ni^{II} complex **12** to the same conditions, which provided the corresponding norcorrole **3** in a higher yield of 76%. Considering that **3** and **4** exhibited similar stability under ambient conditions, the different isolated yields should not be rationalized by the decomposition during the work-up process. We then compared the solubility of **3** and **4** in CHCl$_3$, CH$_2$Cl$_2$, toluene, acetone, and ethyl acetate (Table S1). *meso*-Diphenylnorcorrole **4** displayed 2–10 times lower solubility in comparison to *meso*-dimesitylnorcorrole **4**. Consequently, we hypothesized that the low isolated yield of **3** in the previous procedure was due to the loss of the product during silica-gel chromatography because of its low solubility. After the extensive optimization of the purification steps, we established an improved procedure (Scheme S1, method b). 1) The crude mixture after the reaction of **11** with Ni(cod)$_2$ was passed through a short pad of Celite® with copious washing with CHCl$_3$, removing insoluble materials such as metal salts. 2) The solvent was removed from the filtrate under reduced pressure. 3) The solid residue was washed with acetone. This new protocol afforded analytically pure *meso*-diphenylnorcorrole **4** in 56% (Fig. S6, S7). The byproducts in this reaction were oxacorroles and octaphyrin(1.0.1.0.1.0.1.0).[3] These byproducts exhibit high solubility in common organic solvents due to their low symmetry and high flexibility, thus enabling the separation by washing with acetone.

Table S1 Solubility [g/L] of **3** and **4** in common organic solvents at 25 °C.

Solvent	**3**	**4**
CHCl$_3$	1.2×10	6.2
CH$_2$Cl$_2$	1.0×10	4.4
toluene	5.8	5.1×10^{-1}
acetone	4.0×10^{-1}	4.4×10^{-2}
ethyl acetate	2.5×10^{-2}	1.7×10^{-2}

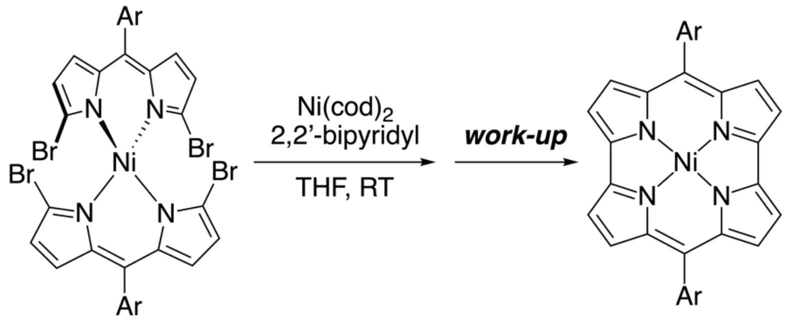

11 (Ar = C_6H_5)
12 (Ar = 2,4,6-$(CH_3)_3C_6H_2$)

4 (Ar = C_6H_5)
3 (Ar = 2,4,6-$(CH_3)_3C_6H_2$)

work-up

method a
1) filtration by alumina, 2) evaporation, and 3) silica-gel chromatography
isolated yields: **3** (76%), **4** (28%)

method b
1) filtration by Celite®, 2) evaporation, and 3) washing with acetone
isolated yield: **4** (56%)

Scheme S1 Improved work-up procedure for the synthesis of *meso*-diphenylnorcorrole **3**.

Ni^{II} *meso*-Dimesitylnorcorrole 3 (Method a)

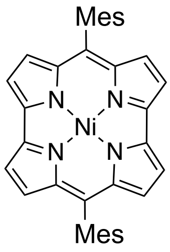

Dipyrrin complex **12** (358.8 mg, 0.40 mmol), bis(1,5-cyclooctadiene)nickel (277.5 mg, 1.00 mmol), and 2,2'-bipyridyl (155.8 mg, 0.40 mmol) were dissolved in degassed and dehydrated THF (22.5 mL) in an argon-filled glovebox. The solution was stirred at room temperature for 3 h under argon. The solution was passed through an alumina pad and evaporated under reduced pressure to provide a solid residue. The residue was purified by silica gel column chromatography (hexane/CH_2Cl_2 = 6/1 as an eluent) to afford **3** in 46% (106 mg, 0.184 mmol) as a green solid.

The compound data was consistent with the reported ones.[3a] ^{1}H NMR ($CDCl_3$, 25 °C): δ 6.26 (s, 4H, Mes), 2.90 (s, 12H, Mes), 1.82 (s, 6H, Mes), 1.57 (d, J = 4.0 Hz, 4H, β-H), 1.47 (d, J = 4.0 Hz, 4H, β-H) ppm; ^{13}C NMR ($CDCl_3$, 25 °C): δ 165.4, 158.7, 148.0, 136.8, 133.3, 129.6, 128.0, 125.7, 114.8, 20.5, 17.5 ppm.

Ni^{II} *meso*-Diphenylnorcorrole 4 (Method b)

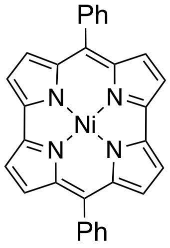

Dipyrrin complex **11** (352 mg, 0.40 mmol), bis(1,5-cyclooctadiene)nickel (275.5 mg, 0.40 mmol), and 2,2'-bipyridyl (155.8 mg, 0.4 mmol) were dissolved in degassed and dehydrated THF (80 mL) in an argon-filled glovebox. The solution was stirred for 3 h at room temperature under argon. The reaction mixture was filtered through a short pad of Celite® ($CHCl_3$ as an eluent). The solvent was removed *in vacuo*. The residue was washed with acetone, which afforded **4** in 54% (106 mg, 0.215 mmol) as a green solid.

The compound data was consistent with the reported ones.[2] ^{1}H NMR ($CDCl_3$, 25 °C): δ 6.89 (t, J = 7.5 Hz, 2H, Ph), 6.68 (t, J = 7.5 Hz, 4H, Ph), 6.00 (d, J = 7.5 Hz, 4H, Ph), 2.20 (d, J = 4.0 Hz, 4H, β-H), 1.84 (d, J = 4.0 Hz, 4H, β-H) ppm; ^{13}C NMR ($CDCl_3$, 25 °C): δ 167.8, 158.6, 147.4, 131.8, 131.0, 131.0, 127.8, 120.3, 114.7 ppm.

Ni^{II} *meso*-Methyl-α,α'-dibromodipyrrin 10

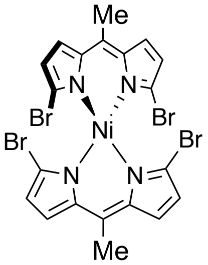

A two-necked flask containing 5-methyldipyrromethane **8** (2.20 g, 13.7 mmol) was evacuated and then refilled with N_2. To the flask, dry THF (100 mL) was added. The solution was cooled to –78 °C. *N*-Bromosuccinimide (4.89 g, 27.4 mmol) was added to the solution in three portions with a 10 min interval. The mixture was stirred for 1 h. To the mixture, 2,3-dichloro-5,6-dicyano-1,4-benzoquinone (DDQ, 3.23 g, 15.1 mmol) was added. After stirred at –78 °C for 1 h, $Ni(OAc)_2 \cdot 4H_2O$ (1.21 g, 6.85 mmol) was added to the solution and warmed to room temperature. After stirred at room temperature for 1 h, the reaction mixture was filtered through a short pad of alumina column (CH_2Cl_2 as an eluent). The solvent was removed under reduced pressure, the residue was purified by silica-gel column chromatography (CH_2Cl_2/hexane = 1/4 as an eluent), which afforded **10** in 11% (532 mg, 7.73 mmol) as a red powder.

HR-MS (ESI-MS): *m/z* = 684.7402, calcd for $(C_{20}H_{14}N_4Br_4Ni)^+$ = 684.7378 $[M + H]^+$. The ^{1}H NMR spectrum was too broad to be assigned because of the paramagnetic nature of **10**.

Ni^{II} *meso*-Dimethylnorcorrole 7

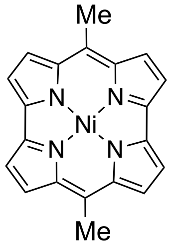

Dipyrrin complex **10** (50 mg, 0.073 mmol), bis(1,5-cyclooctadiene)nickel (20 mg, 0.18 mmol), and 2,2'-bipyridyl (28 mg, 0.18 mmol) were dissolved in dehydrated THF (13 mL) in an argon-filled glovebox. The solution was stirred for 4 h at room temperature under argon. The reaction mixture was filtered through a short pad of Celite® ($CHCl_3$ as an eluent). The solvent was removed *in vacuo*. The residue was purified by silica-gel column chromatography (CH_2Cl_2/hexane = 1/4 as an eluent) and the collected yellow brown band was concentrated, which afforded **7** in 26% (7.0 mg, 19 μmol) as a black powder.

^{1}H NMR ($CDCl_3$, 25 °C): δ 3.11 (d, J = 4.0 Hz, 4H, β-H), 2.42 (d, J = 4.0 Hz, 4H, β-H), –0.96 (s, 6H, methyl) ppm; λ_{max} (ε [M^{-1} cm^{-1}]) = 422 (34000), 504 (17000) nm; HR-MS (ESI-MS): *m/z* = 368.0555, calcd for $(C_{20}H_{14}N_4Ni)^+$ = 368.0566 $[M]^+$. The ^{13}C NMR spectrum was not obtained because of the low solubility of **7**.

3. NMR Spectra

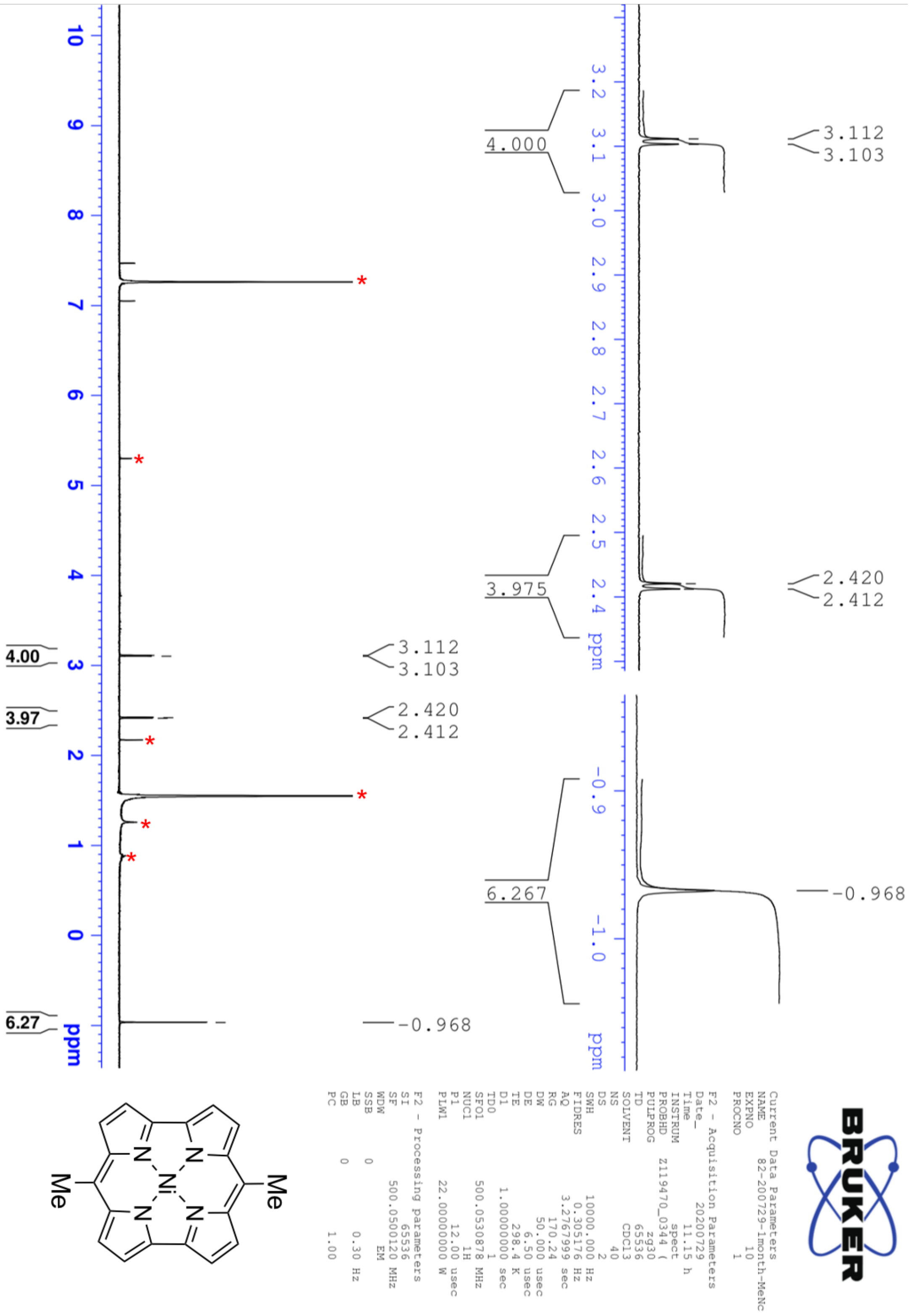

```
Current Data Parameters
NAME      82-200729-1month-MeNc
EXPNO                10
PROCNO                1

F2 - Acquisition Parameters
Date_          20200729
Time              11.15 h
INSTRUM           spect
PROBHD   Z119470_0344 (
PULPROG            zg30
TD                65536
SOLVENT           CDCl3
NS                   40
DS                    2
SWH           10000.000 Hz
FIDRES         0.305176 Hz
AQ            3.2767999 sec
RG               170.24
DW               50.000 usec
DE                 6.50 usec
TE                298.4 K
D1           1.00000000 sec
TD0                   1
SFO1        500.0530878 MHz
NUC1                 1H
P1                12.00 usec
PLW1        22.00000000 W

F2 - Processing parameters
SI                65536
SF          500.0500120 MHz
WDW                  EM
SSB                   0
LB                 0.30 Hz
GB                    0
PC                 1.00
```

Fig. S1 ^{1}H NMR (500 MHz) spectrum of **7** in $CDCl_3$ at 25 °C (*solvent peaks).

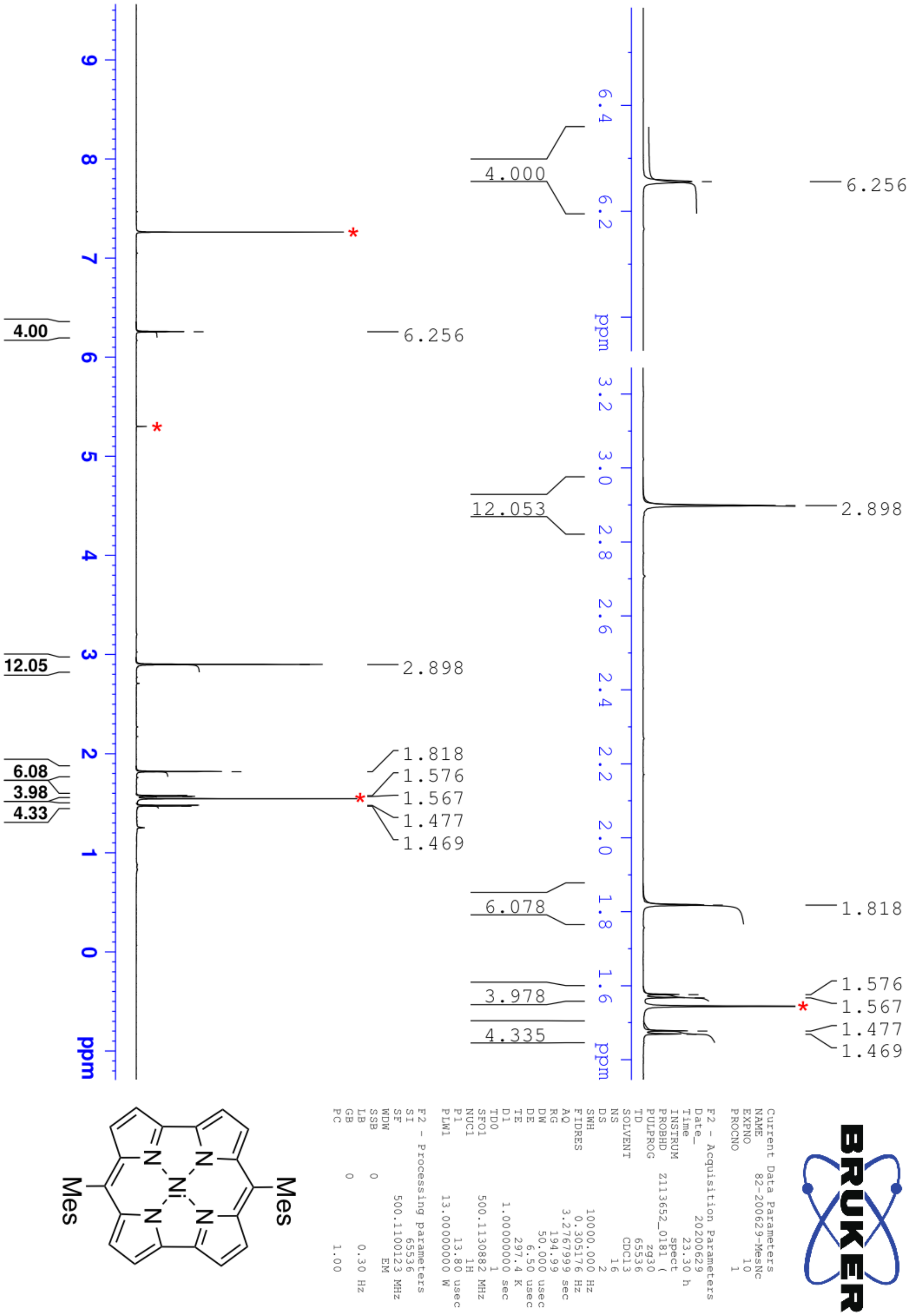

Fig. S2 ^{1}H NMR (500 MHz) spectrum of **3** in $CDCl_3$ at 25 °C (*solvent peaks).

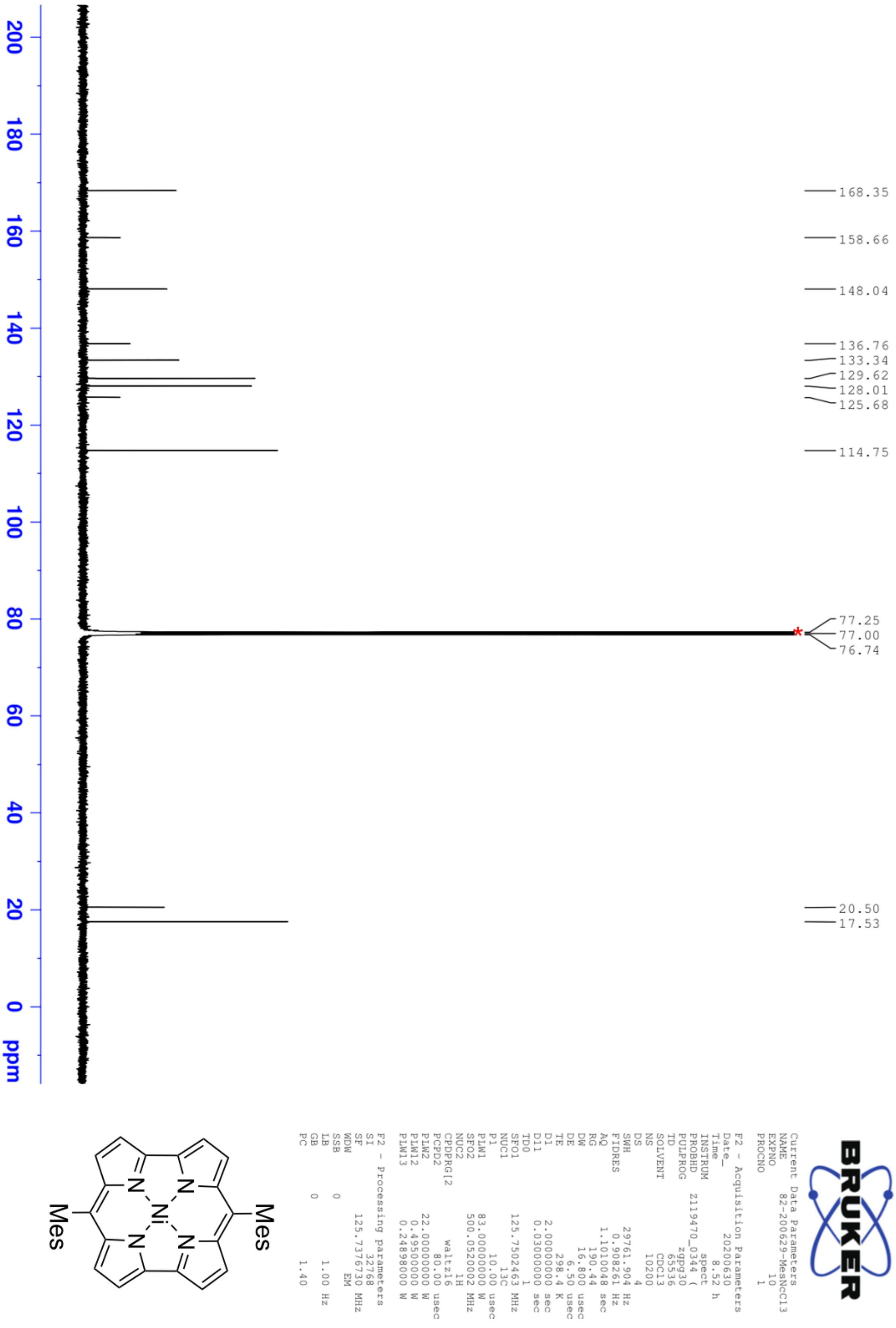

```
Current Data Parameters
NAME        82-200629-MesNcCl3
EXPNO                   10
PROCNO                   1

F2 - Acquisition Parameters
Date_             20200630
Time                  8.52 h
INSTRUM              spect
PROBHD   Z119470_0344 (
PULPROG            zgpg30
TD                   65536
SOLVENT              CDCl3
NS                   10200
DS                       4
SWH              29761.904 Hz
FIDRES            0.908261 Hz
AQ               1.1010048 sec
RG                  190.44
DW                  16.800 usec
DE                    6.50 usec
TE                   298.4 K
D1              2.00000000 sec
D11             0.03000000 sec
TD0                      1
SFO1           125.7502463 MHz
NUC1                   13C
P1                   10.00 usec
PLW1           83.00000000 W
SFO2           500.0520002 MHz
NUC2                    1H
CPDPRG[2           waltz16
PCPD2                80.00 usec
PLW2           22.00000000 W
PLW12           0.49500000 W
PLW13           0.24898000 W

F2 - Processing parameters
SI                   32768
SF             125.7376730 MHz
WDW                     EM
SSB      0
LB                    1.00 Hz
GB       0
PC                    1.40
```

Fig. S3 ^{13}C NMR (500 MHz) spectrum of **3** in $CDCl_3$ at 25 °C (*solvent peaks).

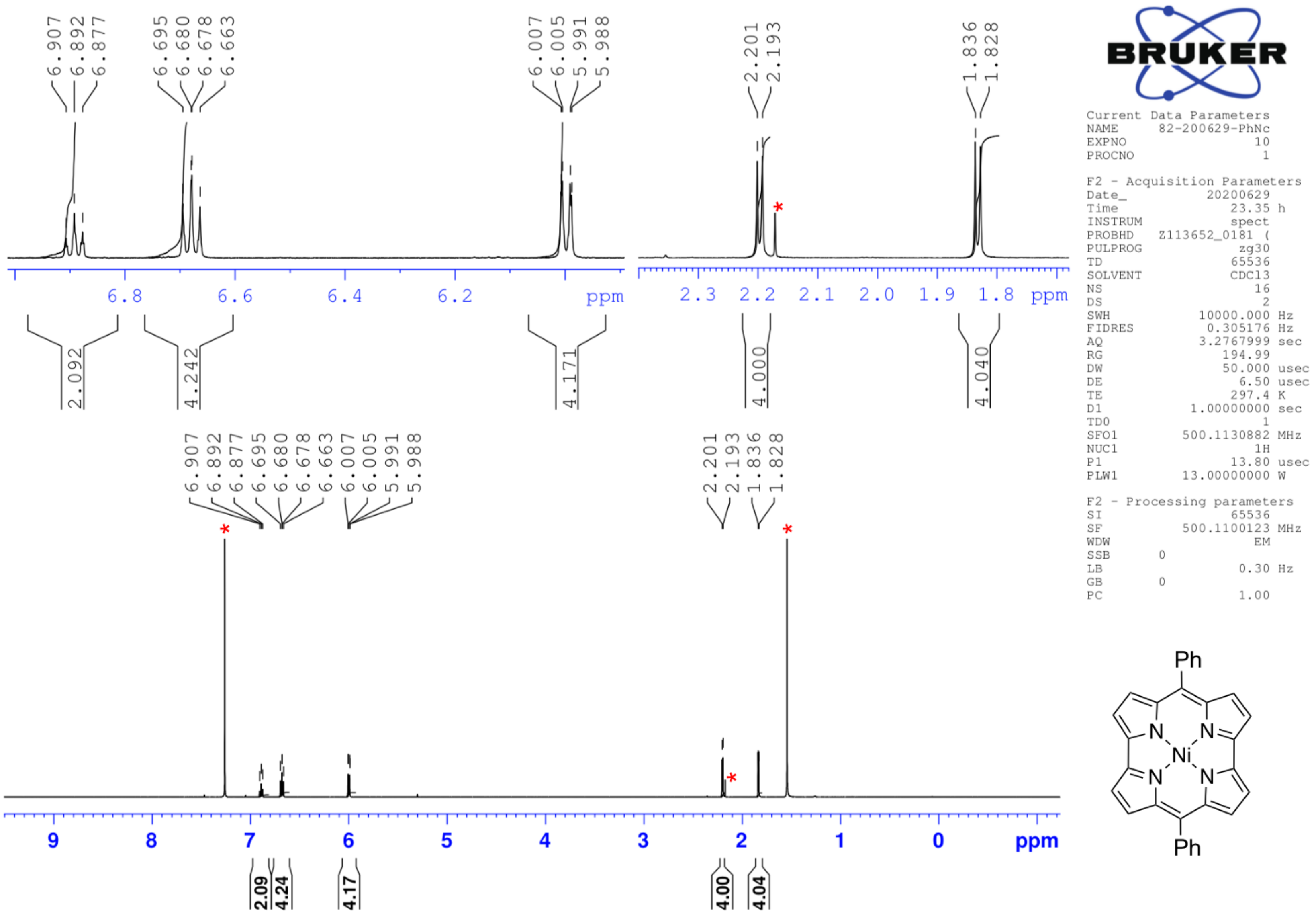

```
Current Data Parameters
NAME     82-200629-PhNc
EXPNO                10
PROCNO                1

F2 - Acquisition Parameters
Date_          20200629
Time              23.35 h
INSTRUM           spect
PROBHD   Z113652_0181 (
PULPROG            zg30
TD                65536
SOLVENT           CDCl3
NS                   16
DS                    2
SWH           10000.000 Hz
FIDRES         0.305176 Hz
AQ            3.2767999 sec
RG               194.99
DW               50.000 usec
DE                 6.50 usec
TE                297.4 K
D1           1.00000000 sec
TD0                   1
SFO1        500.1130882 MHz
NUC1                 1H
P1                13.80 usec
PLW1        13.00000000 W

F2 - Processing parameters
SI                65536
SF          500.1100123 MHz
WDW                  EM
SSB      0
LB                 0.30 Hz
GB       0
PC                 1.00
```

Fig. S4 ^{1}H NMR (500 MHz) spectrum of **4** in $CDCl_3$ at 25 °C (*solvent peaks).

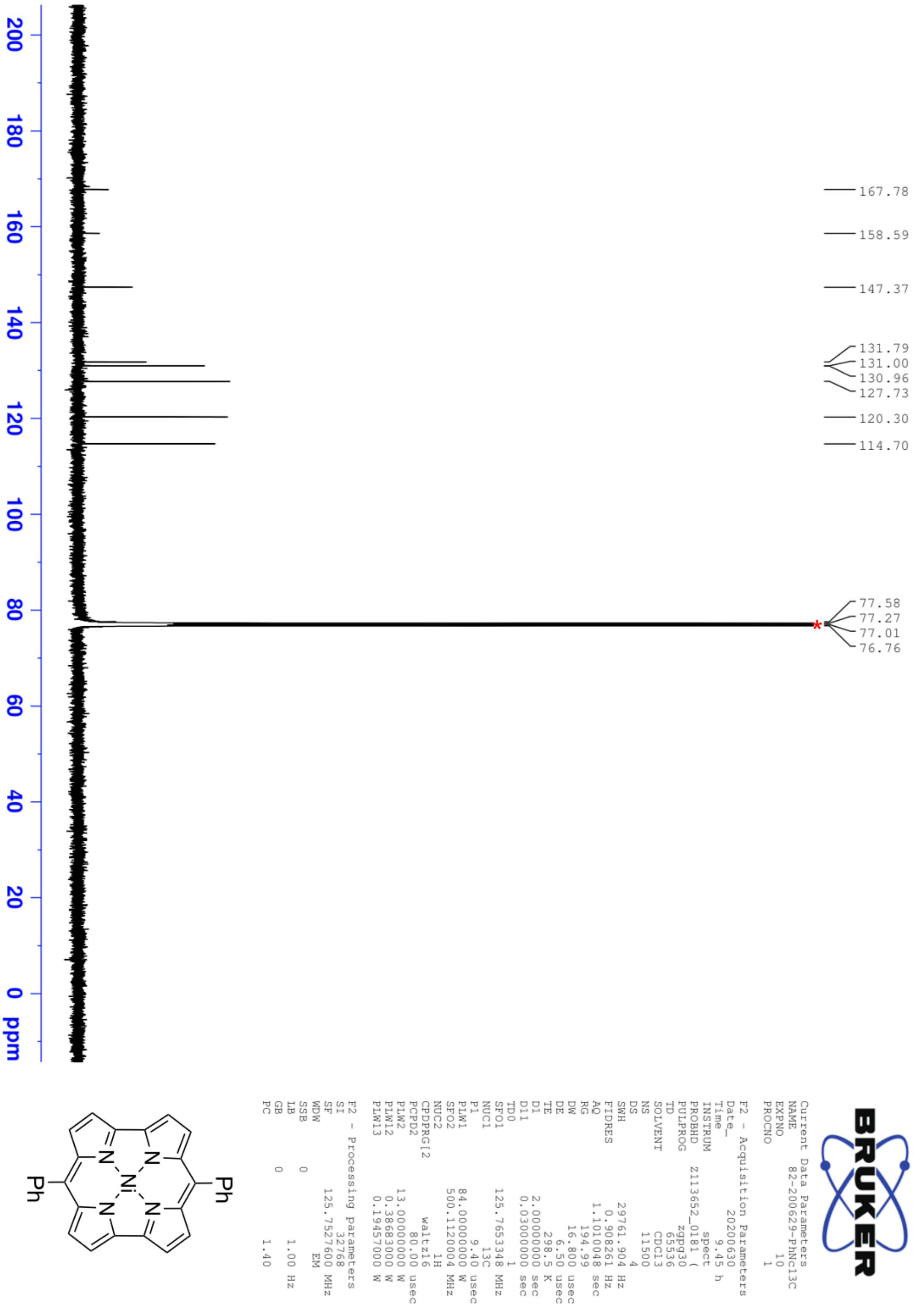

```
Current Data Parameters
NAME      82-200629-PhNc13C
EXPNO                    10
PROCNO                    1

F2 - Acquisition Parameters
Date_              20200630
Time                   9.45 h
INSTRUM               spect
PROBHD   Z113652_0181 (
PULPROG             zgpg30
TD                    65536
SOLVENT               CDCl3
NS                    11500
DS                        4
SWH               29761.904 Hz
FIDRES             0.908261 Hz
AQ                1.1010048 sec
RG                   194.99
DW                   16.800 usec
DE                     6.50 usec
TE                    298.5 K
D1               2.00000000 sec
D11              0.03000000 sec
TD0                       1
SFO1            125.7653348 MHz
NUC1                    13C
P1                     9.40 usec
PLW1            84.00000000 W
SFO2            500.1120004 MHz
NUC2                     1H
CPDPRG[2            waltz16
PCPD2                 80.00 usec
PLW2            13.00000000 W
PLW12            0.38683000 W
PLW13            0.19457000 W

F2 - Processing parameters
SI                    32768
SF              125.7527600 MHz
WDW                      EM
SSB      0
LB                     1.00 Hz
GB       0
PC                     1.40
```

Fig. S5 ^{13}C NMR (500 MHz) spectrum of **4** in CDCl$_3$ at 25 °C (*solvent peaks).

4. Purity of Ni(II) Diphenylnorcorrole Provided by Method b

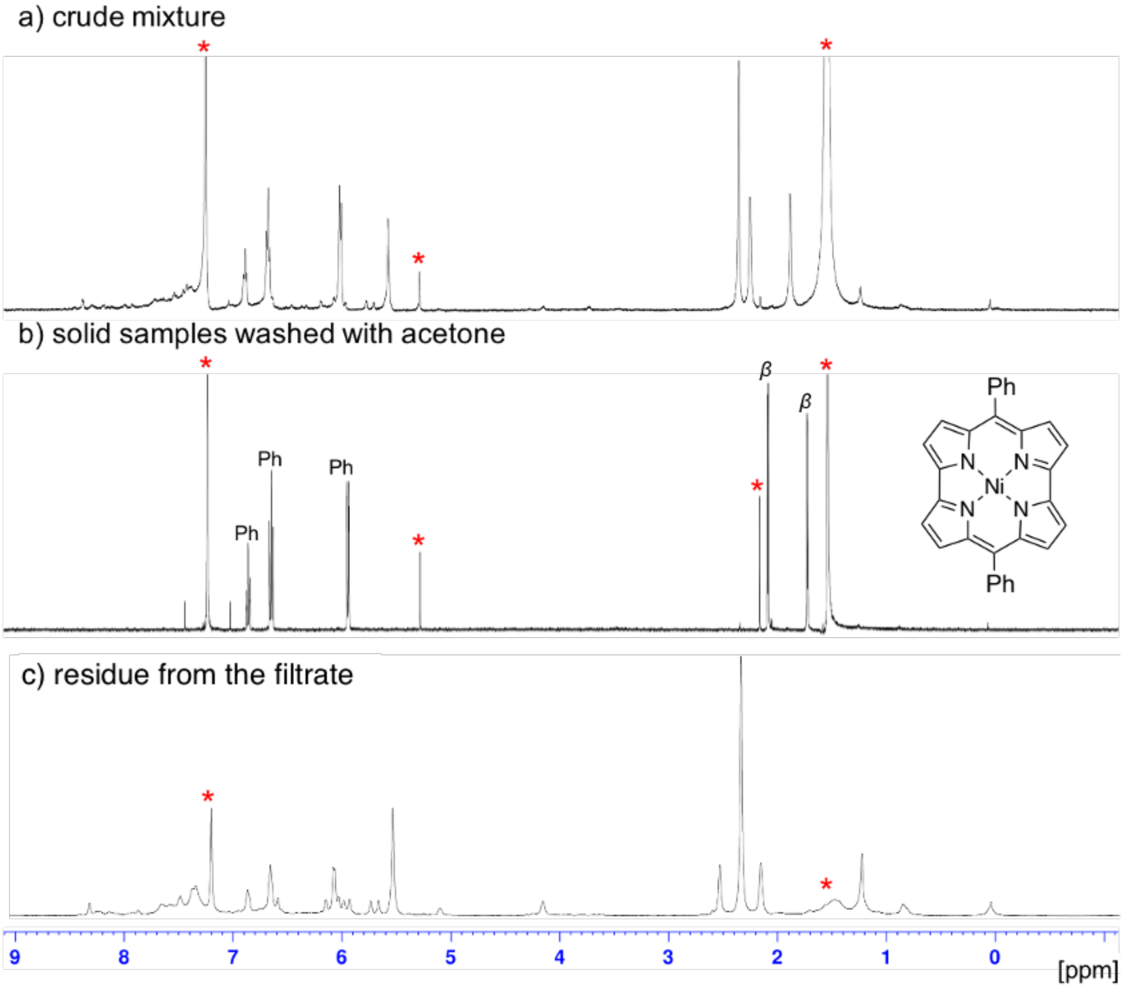

Fig. S6 ^{1}H NMR (500 MHz) spectra of (a) crude mixture, (b) solid samples washed with acetone, and (c) residue from the filtrate in $CDCl_3$ at 25 °C (*solvent peaks).

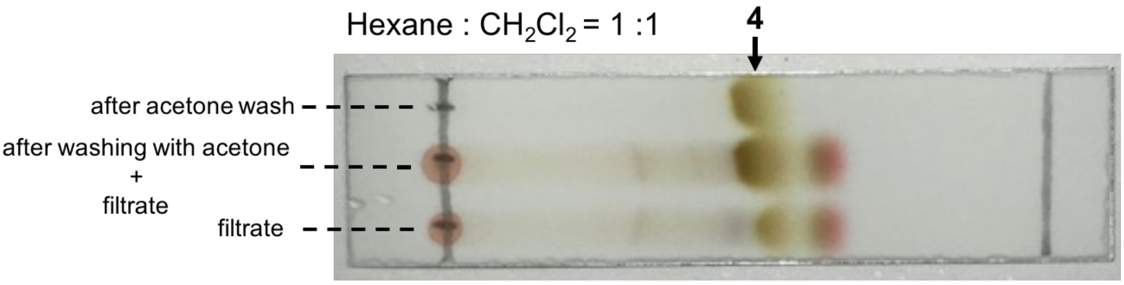

Fig. S7 TLC analysis of solid samples washed with acetone and the residue from the filtrate.

5. Stability of Ni(II) Dimesityl- and Diphenylnorcorroles in Solid

The solid samples of **3** and **4** were prepared on January 21, 2020 and April 20, 2020, respectively. These samples were stored under ambient conditions for 4 and 2 months, respectively. No significant changes were observed by the ^{1}H NMR analysis.

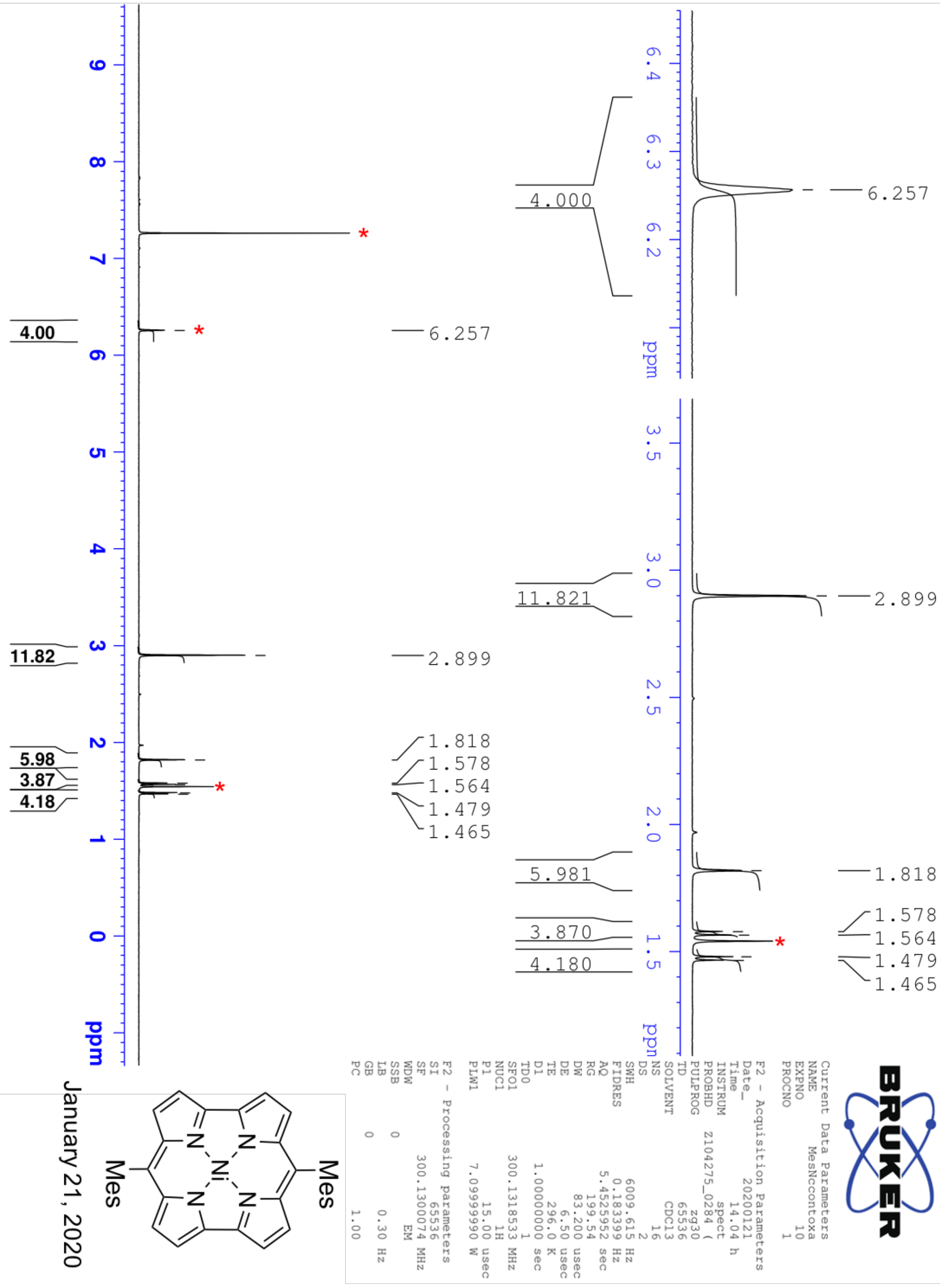

Fig. S8 ^{1}H NMR (500 MHz) spectrum of **3** in $CDCl_3$ at 25 °C on January 21, 2020 (*solvent peaks).

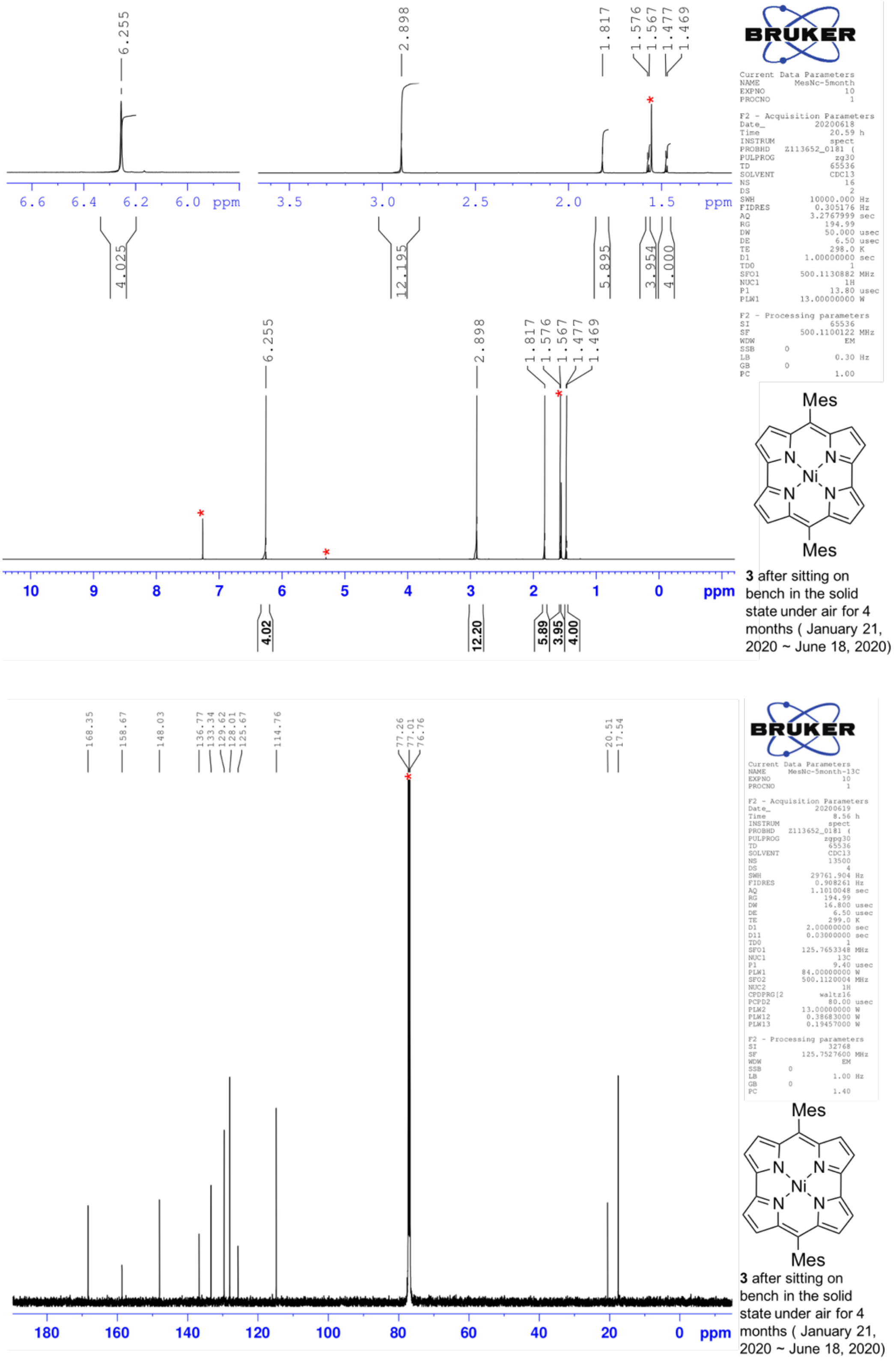

```
Current Data Parameters
NAME          MesNc-5month
EXPNO                   10
PROCNO                   1

F2 - Acquisition Parameters
Date_             20200618
Time                 20.59 h
INSTRUM              spect
PROBHD    Z113652_0181 (
PULPROG               zg30
TD                   65536
SOLVENT              CDCl3
NS                      16
DS                       2
SWH              10000.000 Hz
FIDRES            0.305176 Hz
AQ               3.2767999 sec
RG                  194.99
DW                  50.000 usec
DE                    6.50 usec
TE                   298.0 K
D1              1.00000000 sec
TD0                      1
SFO1           500.1130882 MHz
NUC1                    1H
P1                   13.80 usec
PLW1           13.00000000 W

F2 - Processing parameters
SI                   65536
SF             500.1100122 MHz
WDW                     EM
SSB       0
LB                    0.30 Hz
GB        0
PC                    1.00
```

3 after sitting on bench in the solid state under air for 4 months (January 21, 2020 ~ June 18, 2020)

```
Current Data Parameters
NAME      MesNc-5month-13C
EXPNO                   10
PROCNO                   1

F2 - Acquisition Parameters
Date_             20200619
Time                  8.56 h
INSTRUM              spect
PROBHD    Z113652_0181 (
PULPROG            zgpg30
TD                   65536
SOLVENT              CDCl3
NS                   13500
DS                       4
SWH              29761.904 Hz
FIDRES            0.908261 Hz
AQ               1.1010048 sec
RG                  194.99
DW                  16.800 usec
DE                    6.50 usec
TE                   299.0 K
D1              2.00000000 sec
D11             0.03000000 sec
TD0                      1
SFO1           125.7653348 MHz
NUC1                   13C
P1                    9.40 usec
PLW1           84.00000000 W
SFO2           500.1120004 MHz
NUC2                    1H
CPDPRG[2           waltz16
PCPD2                80.00 usec
PLW2           13.00000000 W
PLW12           0.38683000 W
PLW13           0.19457000 W

F2 - Processing parameters
SI                   32768
SF             125.7527600 MHz
WDW                     EM
SSB       0
LB                    1.00 Hz
GB        0
PC                    1.40
```

3 after sitting on bench in the solid state under air for 4 months (January 21, 2020 ~ June 18, 2020)

Fig. S9 ^{1}H NMR (500 MHz) and ^{13}C NMR (126 MHz) spectra of **3** in $CDCl_3$ at 25 °C on June 18, 2020 (*solvent peaks).

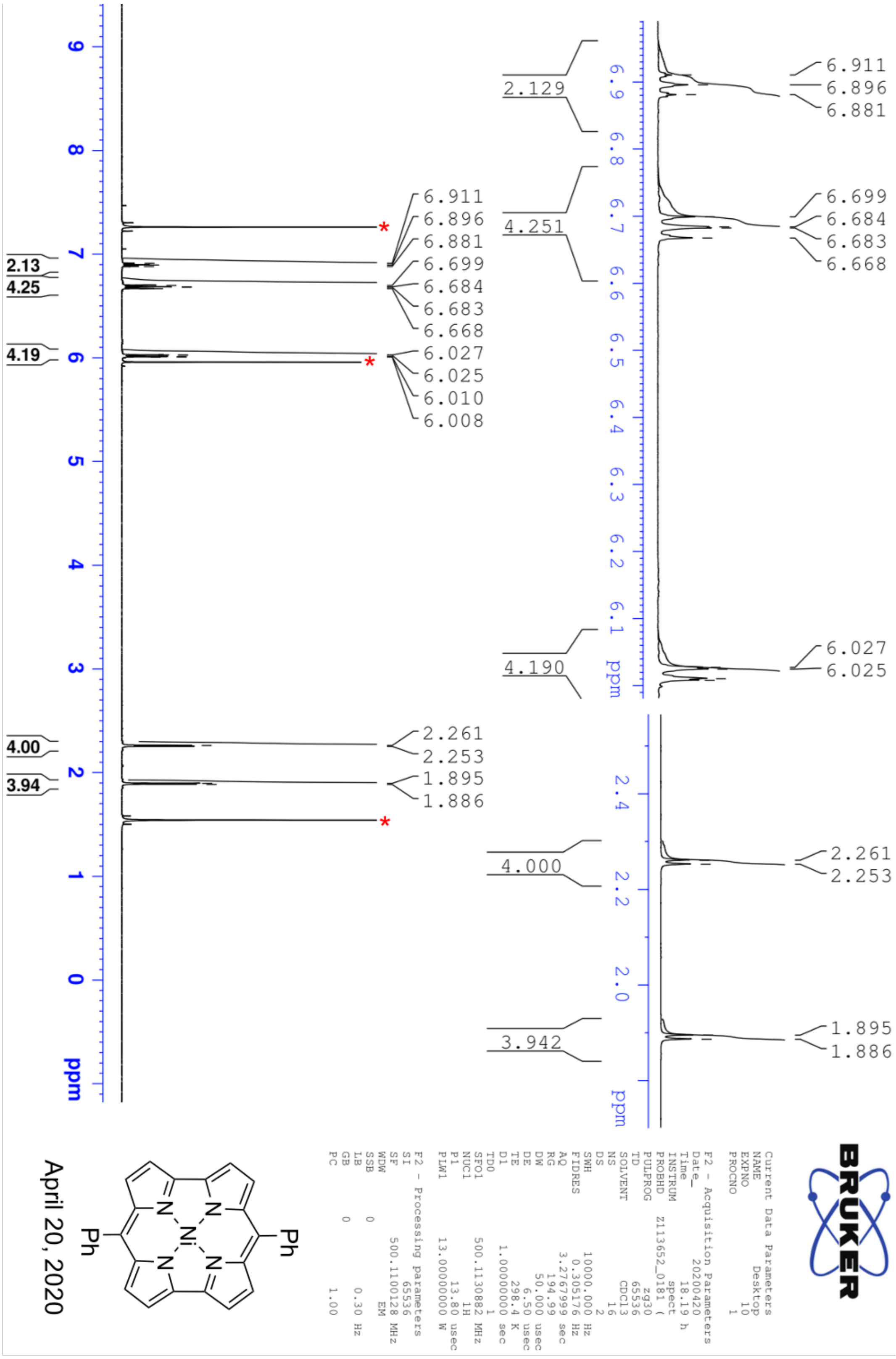

Fig. S10 ^{1}H NMR (500 MHz) spectrum of **4** in $CDCl_3$ at 25 °C on April 20, 2020 (*solvent peaks).

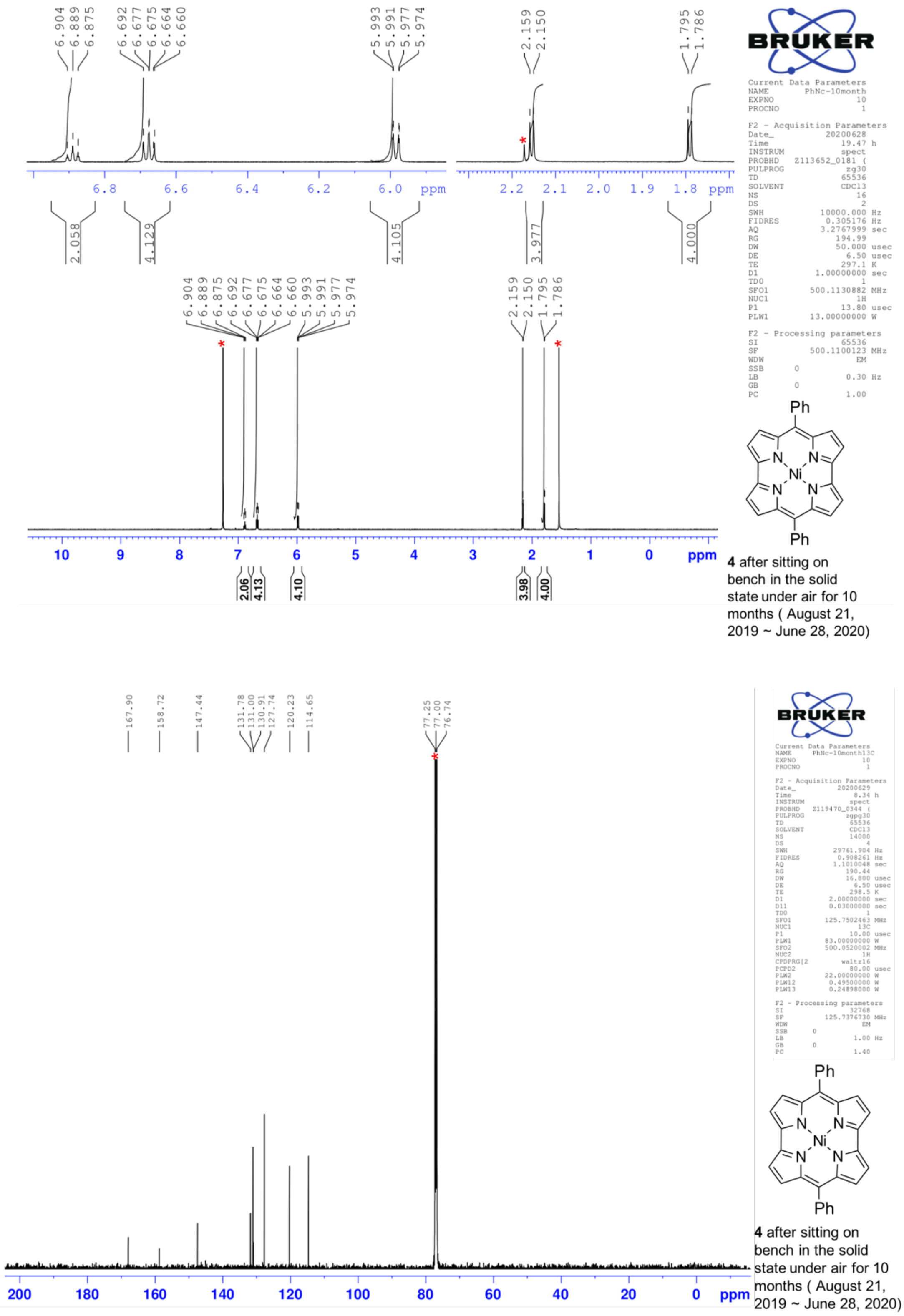

4 after sitting on bench in the solid state under air for 10 months (August 21, 2019 ~ June 28, 2020)

4 after sitting on bench in the solid state under air for 10 months (August 21, 2019 ~ June 28, 2020)

Fig. S11 ^{1}H NMR (500 MHz) and ^{13}C NMR (126 MHz) spectra of **4** in $CDCl_3$ at 25 °C on June 28, 2020 (*solvent peaks).

6. Stability of Ni(II) Dimesityl- and Diphenylnorcorroles in Solution

The $CDCl_3$ solution of **3** or **4** including 1,1,2,2-tetrachloroethane as an internal standard in an NMR tube was let stand for 1 week under ambient conditions. The changes in the ^1H NMR spectra were monitored (Fig. S12 and S13). The decay of the intensity of the signals of **3** or **4** is summarized in Table S2.

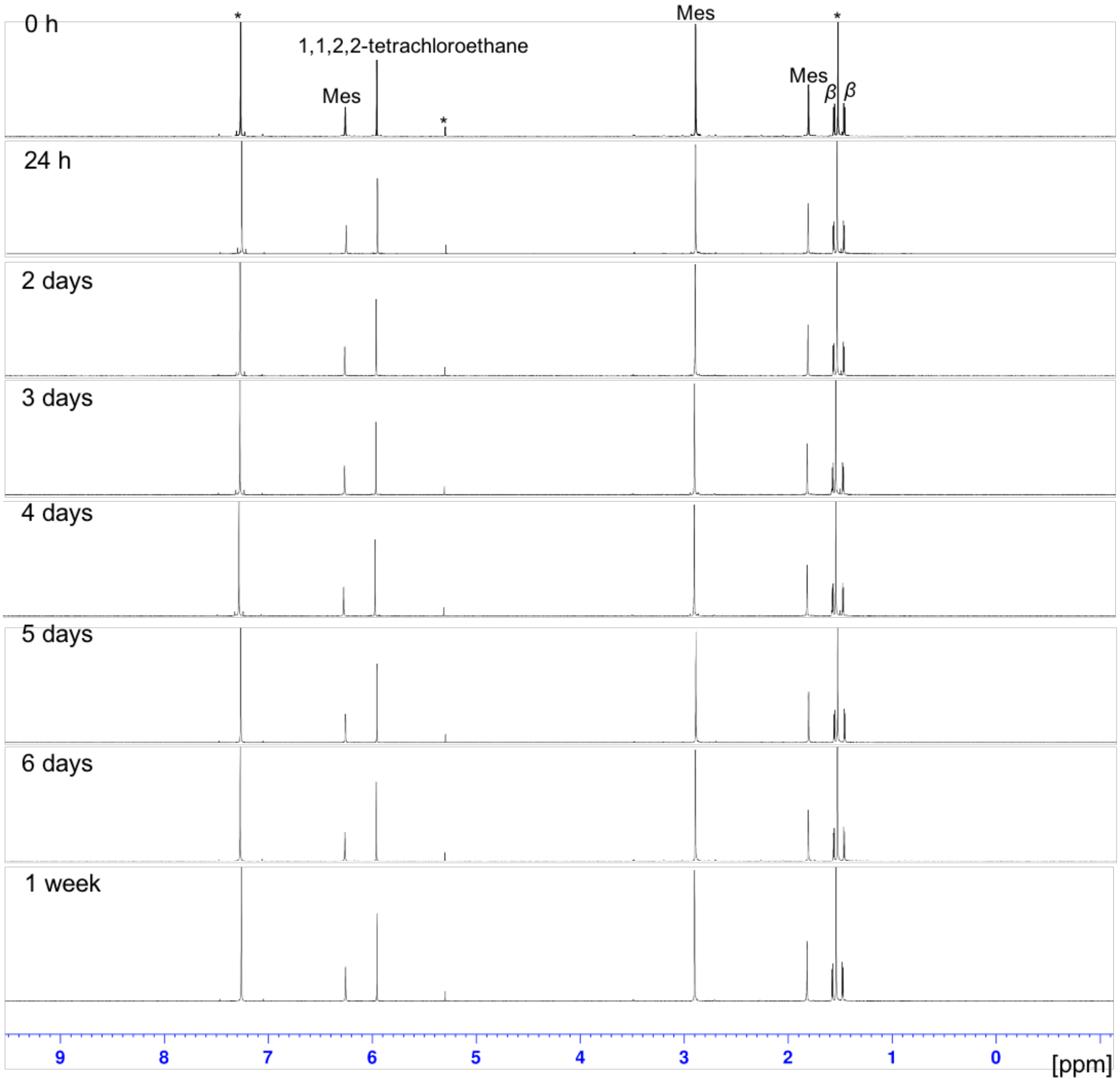

Fig. S12 Change of ^1H NMR (500 MHz) spectra of **3** in $CDCl_3$ at 25 °C (*solvent peaks).

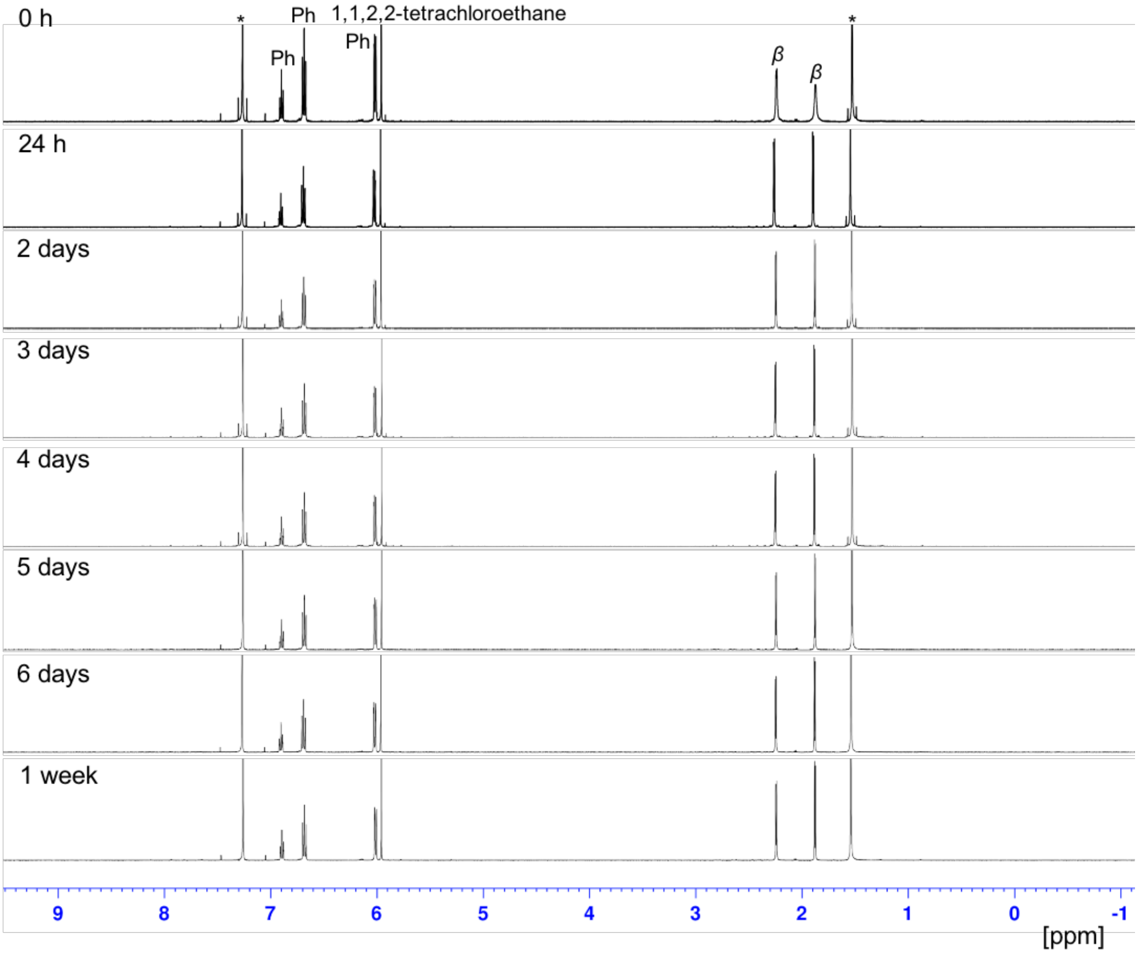

Fig. S13 Change of ^{1}H NMR (500 MHz) spectra of **4** in $CDCl_3$ at 25 °C (*solvent peaks).

Table S2 The relative integrated intensities[a] of the ^{1}H NMR signals of **3** and **4**.

Time	**3** β proton (1.57 ppm)	**4** β proton (2.24 ppm)
0 h	1.13	1.19
24 h	1.13	1.23
2 days	1.19	1.22
3 days	1.13	1.20
4 days	1.12	1.20
5 days	1.11	1.18
6 days	1.11	1.17
1 week	1.11	1.17

[a] These values were calculated on the basis of the integral values of the signal of the internal standard (1,1,2,2-tetrachloroethane).

7. Stability of Ni(II) Dimesityl- and Diphenylnorcorroles to Moisture

The CH_2Cl_2 solution of **3** (1.0 mM, 6.5 mL) and water (40 mL) ware poured into a separatory funnel and shaken vigorously. The organic layer was extracted with CH_2Cl_2 (6.5 mL) and dried over anhydrous sodium sulfate. The solvent was removed *in vacuo*. The residue was dissolved in $CDCl_3$ along with 1,1,2,2-tetrachloroethane as an internal standard. The ^1H NMR yield based was 94%, indicating the almost quantitative recovery of **3**.

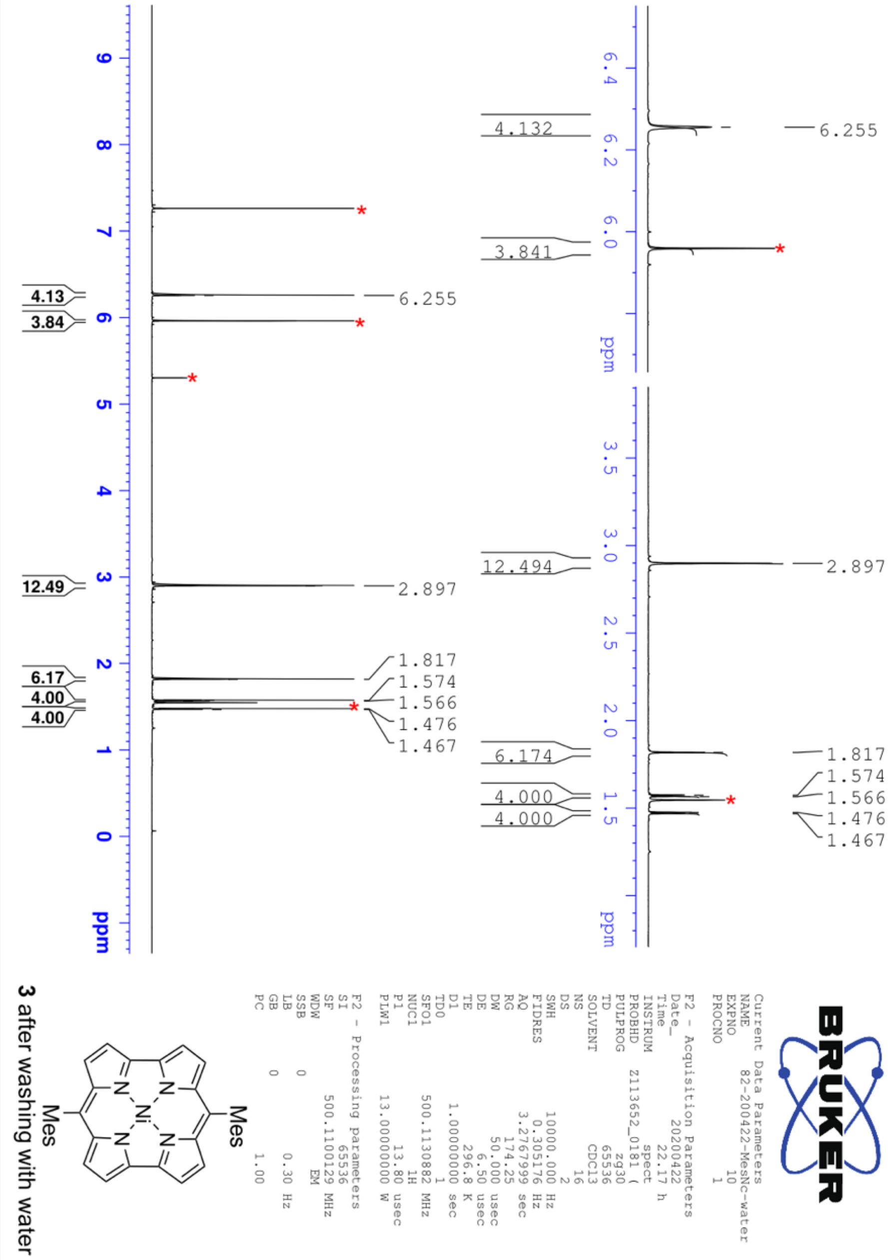

```
Current Data Parameters
NAME      82-200422-MesNc-water
EXPNO                  10
PROCNO                  1

F2 - Acquisition Parameters
Date_            20200422
Time              22.17 h
INSTRUM             spect
PROBHD   Z113652_0181 (
PULPROG              zg30
TD                  65536
SOLVENT             CDCl3
NS                     16
DS                      2
SWH            10000.000 Hz
FIDRES          0.305176 Hz
AQ             3.2767999 sec
RG                 174.25
DW                 50.000 usec
DE                   6.50 usec
TE                  296.8 K
D1            1.00000000 sec
TD0                     1
SFO1          500.1130882 MHz
NUC1                   1H
P1                  13.80 usec
PLW1          13.00000000 W

F2 - Processing parameters
SI                  65536
SF            500.1100129 MHz
WDW                    EM
SSB      0
LB                   0.30 Hz
GB       0
PC                   1.00
```

Fig. S14 ^1H NMR (500 MHz) spectrum of **3** (after washing) in $CDCl_3$ at 25 °C (*solvent peaks).

The CH_2Cl_2 solution of **4** (1.0 mM, 6.5 mL) and water (40 mL) ware poured into a separatory funnel and shaken vigorously. The organic layer was extracted with CH_2Cl_2 (6.5 mL) and dried over anhydrous sodium sulfate. The solvent was removed *in vacuo*. The residue was dissolved in $CDCl_3$ along with 1,1,2,2-tetrachloroethane as an internal standard. The ^{1}H NMR yield was 94%, indicating the almost quantitative recovery of **4**.

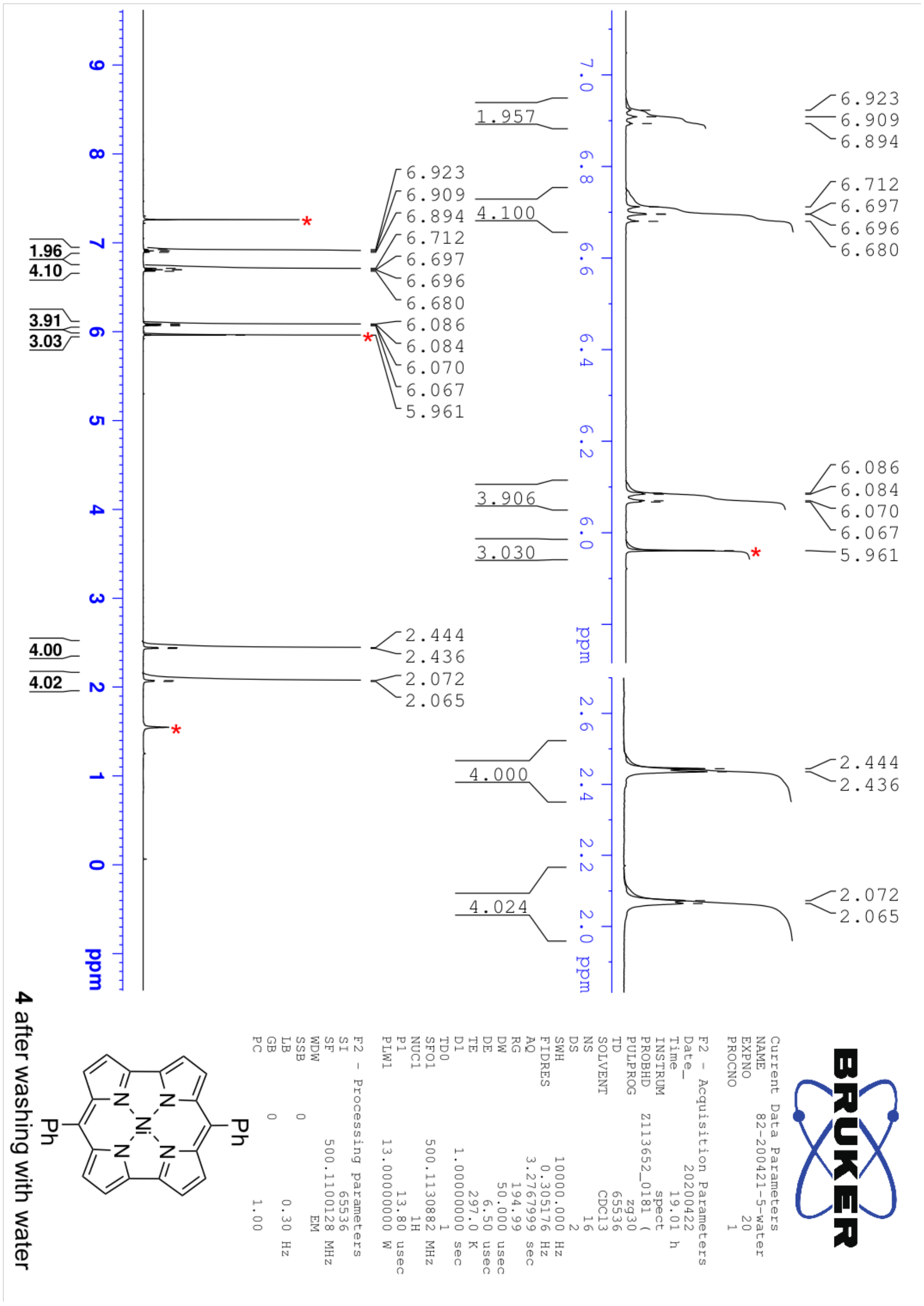

Fig. S15 ^{1}H NMR (500 MHz) spectrum of **4** (after washing) in $CDCl_3$ at 25 °C (*solvent peaks).

8. Stability of Ni(II) Dimesityl- and Diphenylnorcorroles to Silica-Gel

Dimesitylnorcorrole **3** was dissolved in CH_2Cl_2 (5 mL) and loaded onto a plug of silica gel packed with CH_2Cl_2. After elution with CH_2Cl_2, the blown fraction collected into a 20-mL vial and concentrated. The residue was dissolved in $CDCl_3$ along with 1,1,2,2-tetrachloroethane as an internal standard. The ^{1}H NMR yield was 98%, indicating the almost quantitative recovery of **3**.

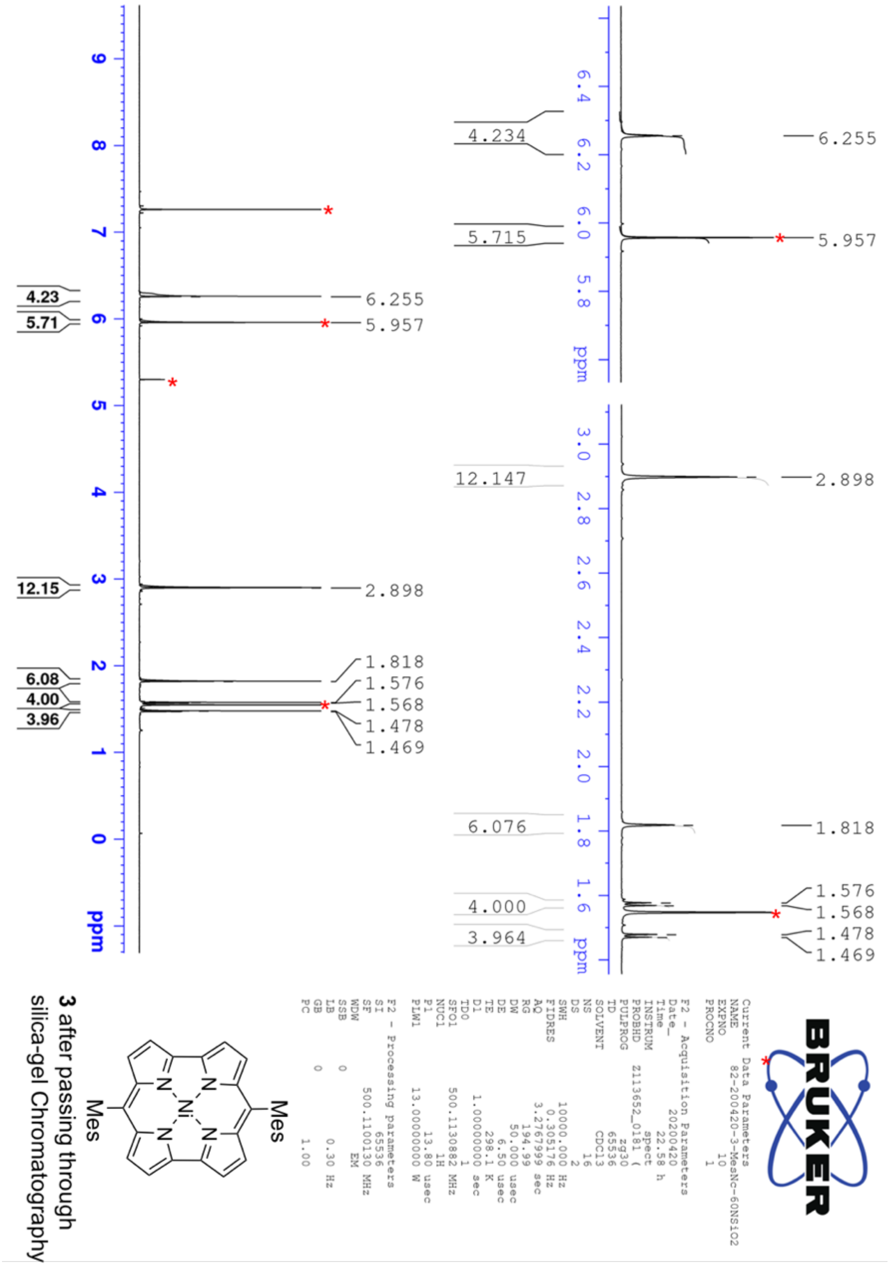

Fig. S16 ^{1}H NMR (500 MHz) spectra of **3** after passing through silica gel in $CDCl_3$ at 25 °C (*solvent peaks).

Diphenylnorcorrole **4** was dissolved in CH_2Cl_2 (5 mL) and loaded onto a plug of silica gel packed with CH_2Cl_2. After elution with CH_2Cl_2, the blown fraction collected into a 20-mL vial and concentrated. The residue was dissolved in $CDCl_3$ along with 1,1,2,2-tetrachloroethane as an internal standard. The ^1H NMR yield was 99%, indicating the almost quantitative recovery of **4**.

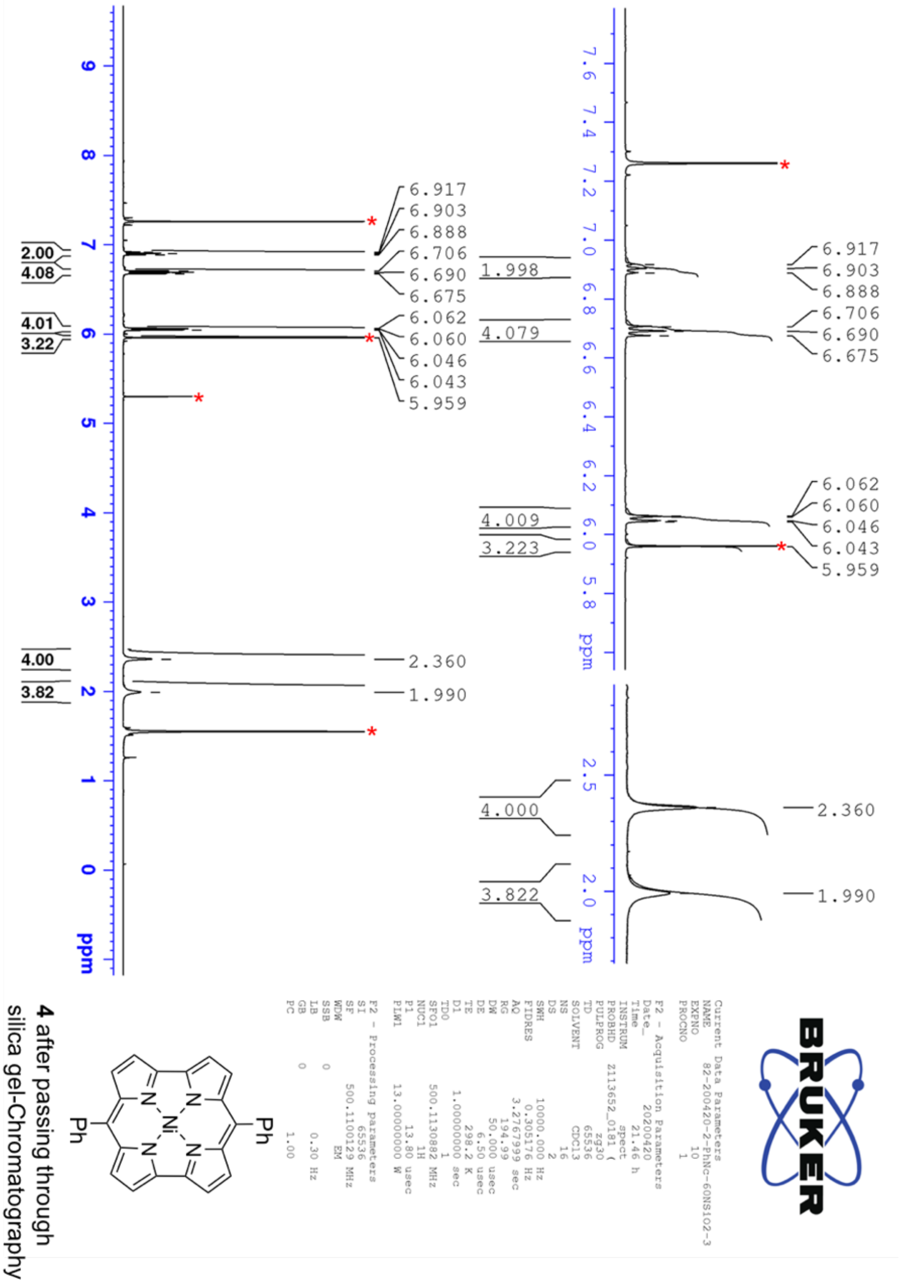

Fig. S17 ^1H NMR (500 MHz) spectra of **4** after passing through silica gel in $CDCl_3$ at 25 °C (*solvent peaks).

9. Stability of Ni(II) Dimesityl- and Diphenylnorcorroles under Air

To a 30-mL flask was add **3** (5.3 mg) and toluene (5.2 mL). The solution was heated to 80 °C for 16 h in air. After 16 h, toluene was removed *in vacuo*. The residue was dissolved in $CDCl_3$ along with 1,1,2,2-tetrachloroethane as an internal standard. The ^1H NMR yield was 96%, indicating the almost quantitative recovery of **3**.

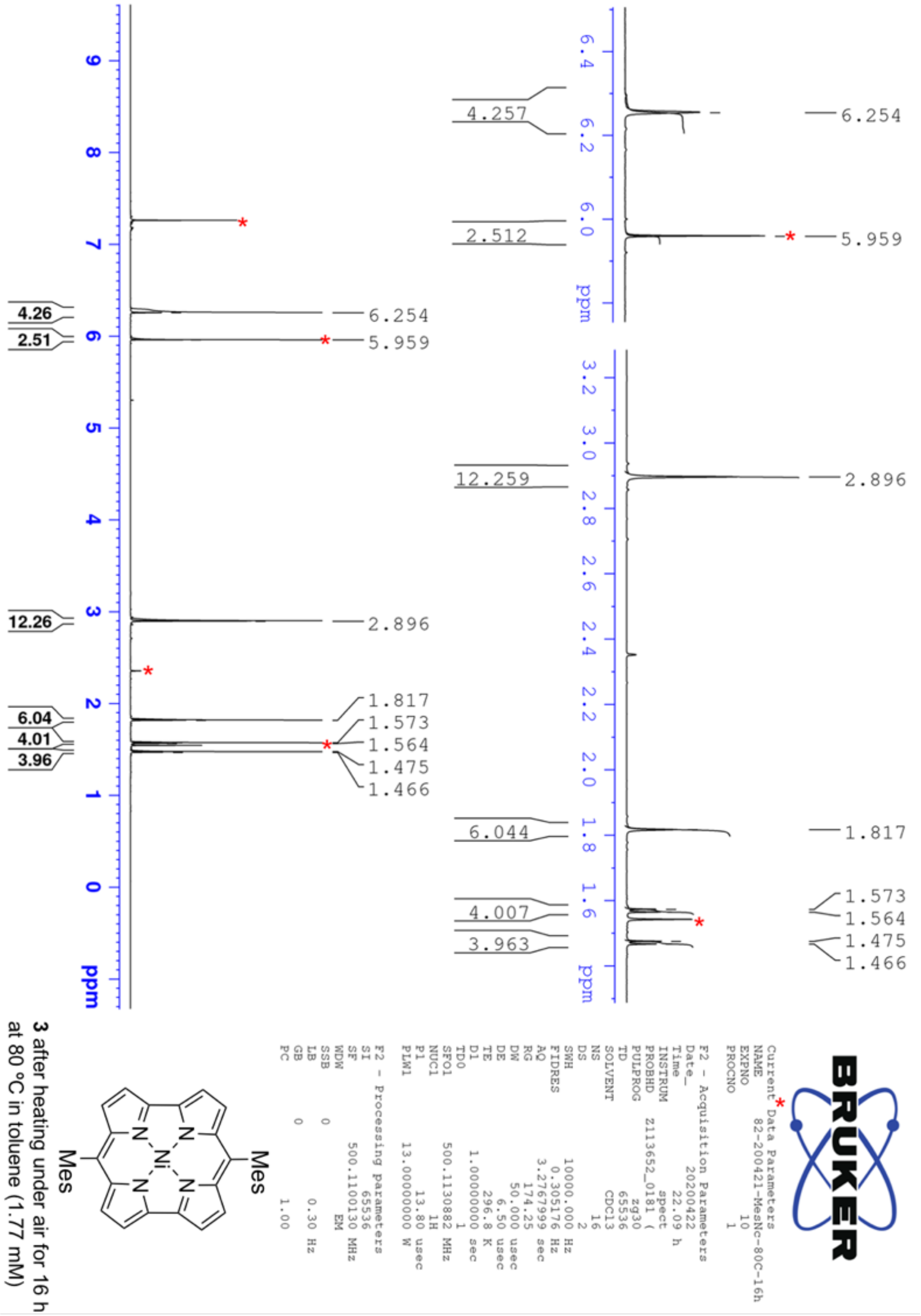

Fig. S18 ^1H NMR (500 MHz) spectra of **3** (after heating) in $CDCl_3$ at 25 °C (*solvent peaks).

To a 30-mL flask was add **4** (2.15 mg, 4.36 μmol) and toluene (5.0 mL). The solution was heated to 80 °C for 16 h in air. After 16 h, toluene was removed *in vacuo*. The residue was dissolved in $CDCl_3$ along with 1,1,2,2-tetrachloroethane as an internal standard. The ^1H NMR yield was 97%, indicating the almost quantitative recovery of **4**.

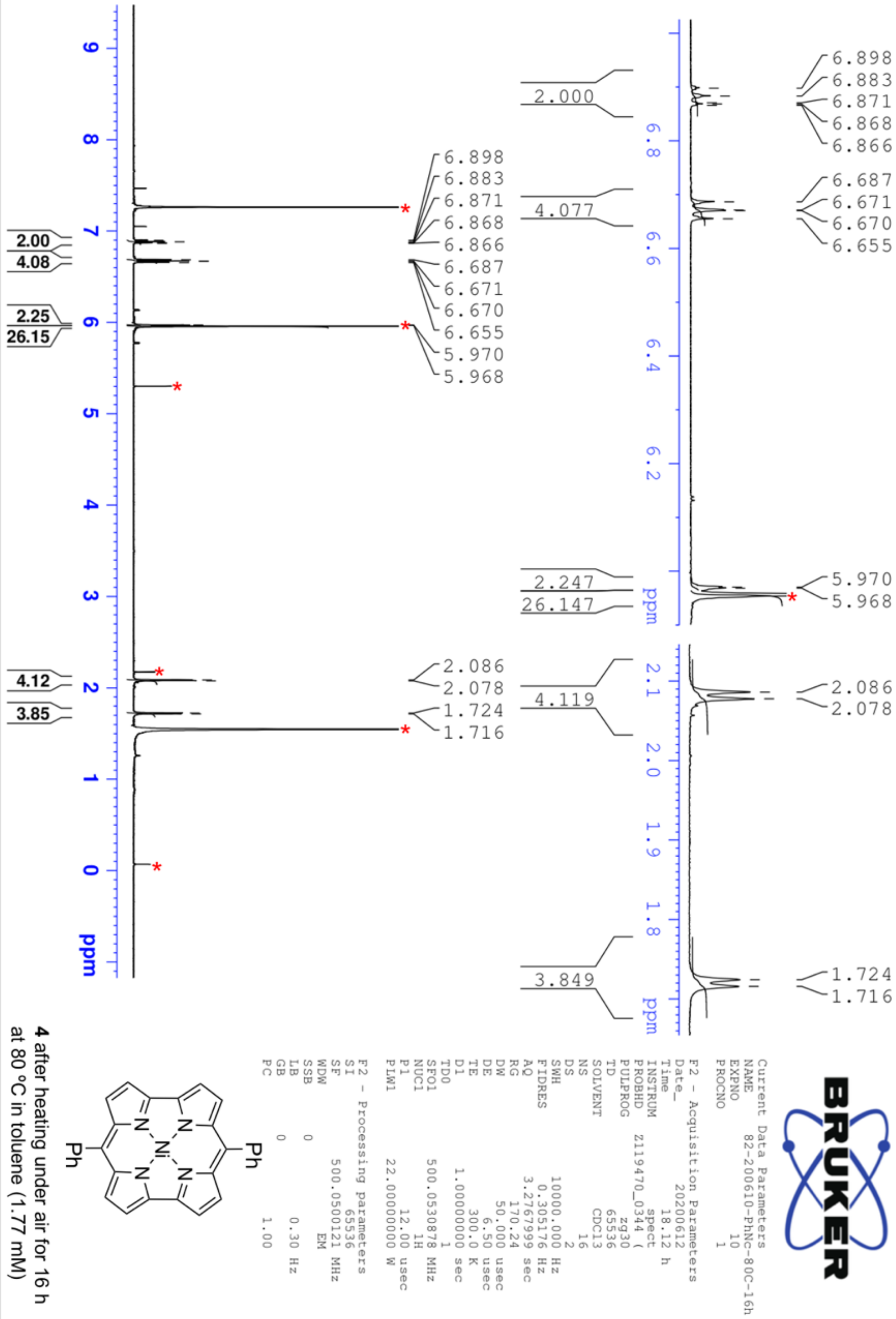

Fig. S19 ^1H NMR (500 MHz) spectra of **4** (after heating) in $CDCl_3$ at 25 °C (*solvent peaks).

10. Stability of Ni(II) Dimethylnorcorrole

Stability in solution

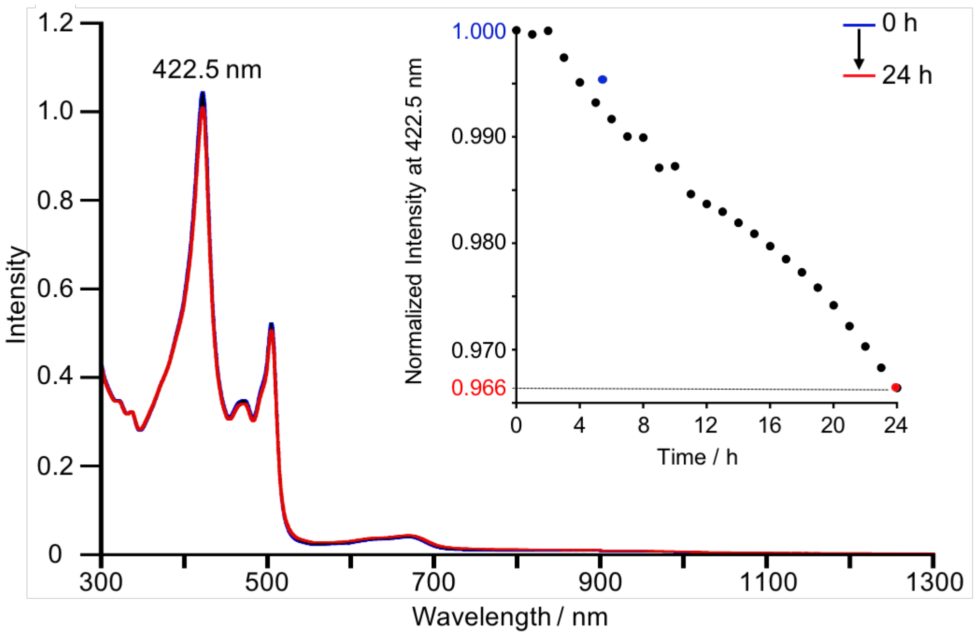

Fig. S20 Time-dependent change in UV/vis/NIR absorption spectra of **7** in CH_2Cl_2 at 25 °C. Inset shows the plots of the intensities at 422.5 nm.

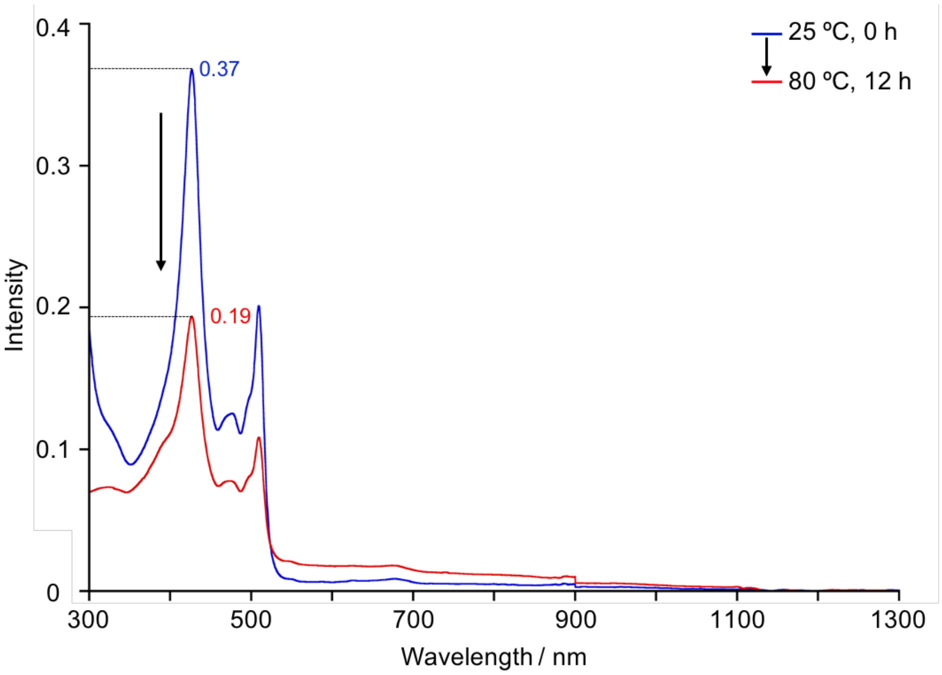

Fig. S21 UV/vis/NIR absorption spectrum of **7** in toluene at 25 °C at 0 min and after heating for 12 h at 80 °C.

Stability in the solid state

The solid sample of **7** was prepared on June 21, 2020. The sample was stored under ambient conditions for 1 month. No significant changes were observed.

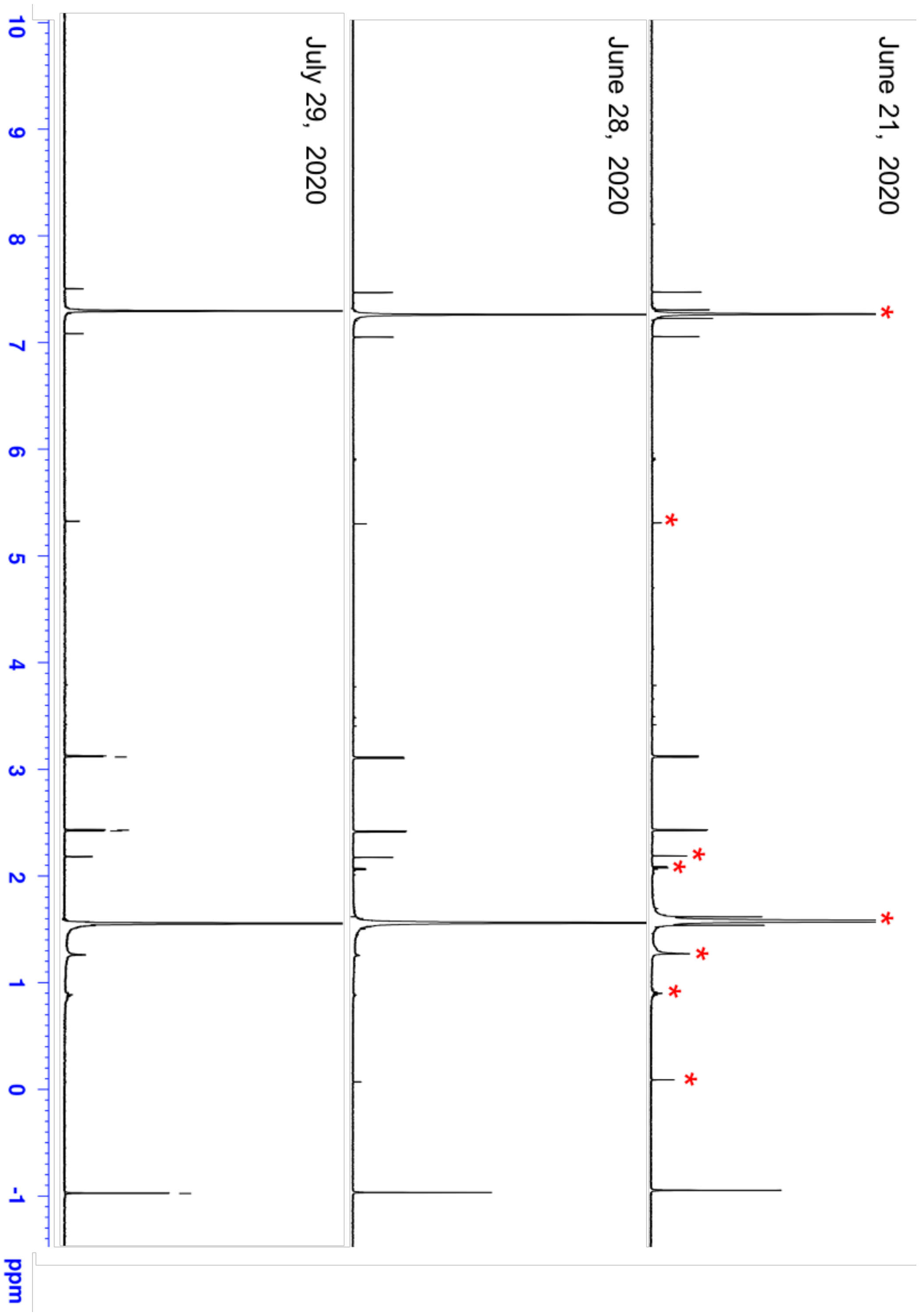

Fig. S22 ^{1}H NMR (500 MHz) spectra of **7** in CDCl$_3$ at 25 °C (*solvent peaks).

11. X-ray Diffraction Analysis

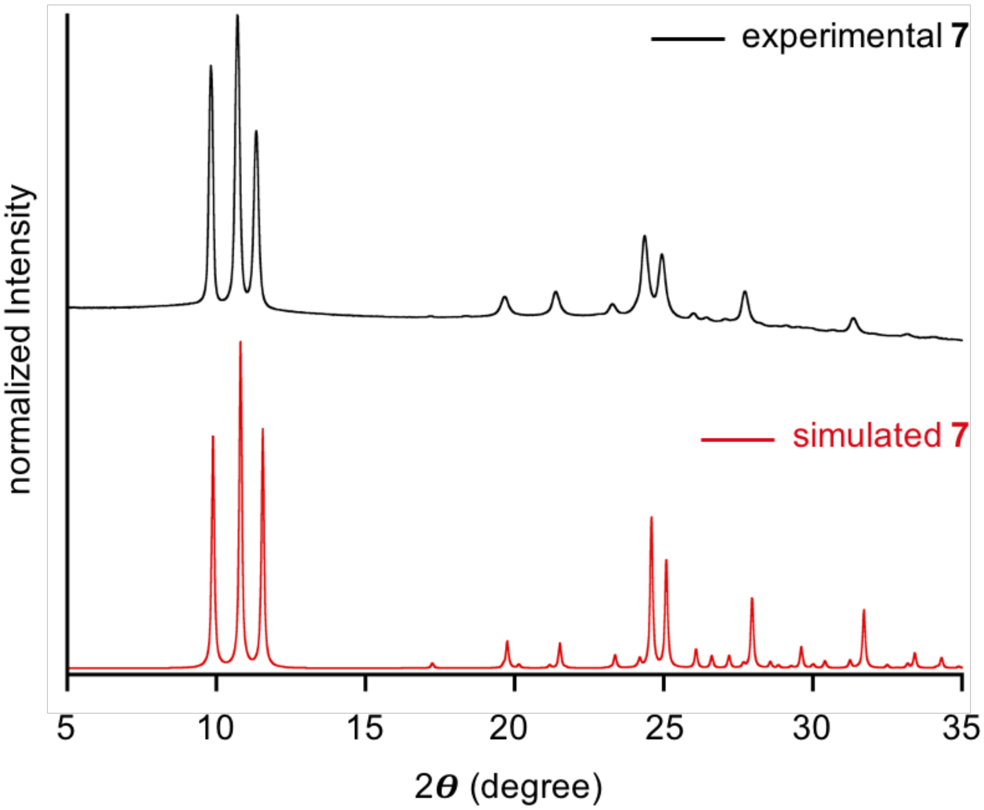

Fig. S23 Experimental (black) and simulated (red) powder X-ray diffraction patterns of **7**.

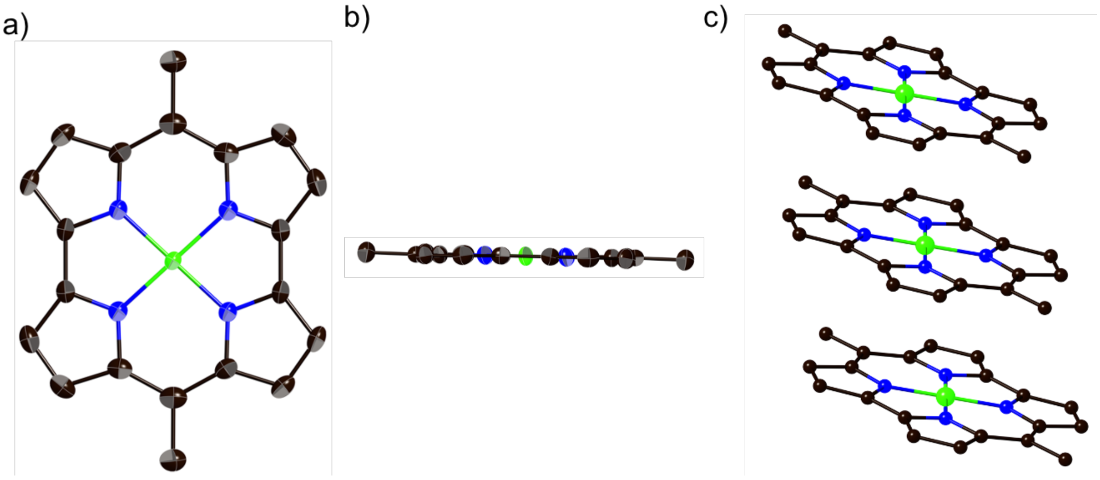

Fig. S24 X-ray crystal structure of **7**. a) Top view, b) side view, and c) packing structure. Thermal ellipsoids are drawn at the 50% probability level. All hydrogen atoms are omitted for clarity.

Table S3 Crystallographic data of **7**.

Compound	**7**
Empirical Formula	$C_{10}H_7N_2Ni_{0.5}$
Mw	369.05
Crystal System	monoclinic
Space Group	*I*12/*a*1 (No. 15)
a	19.3223(7) Å
b	4.6693(1) Å
c	17.6807(6) Å
β	112.336(4)°
Volume	1475.50(9) Å^3
Z	8
Density (calcd.)	1.661 g/cm^{-3}
Completeness	0.993
Goodness-of-Fit	1.076
$R_1[I>2\sigma(I)]$	0.0450
wR_2 (all data)	0.1253
CCDC No.	2020183

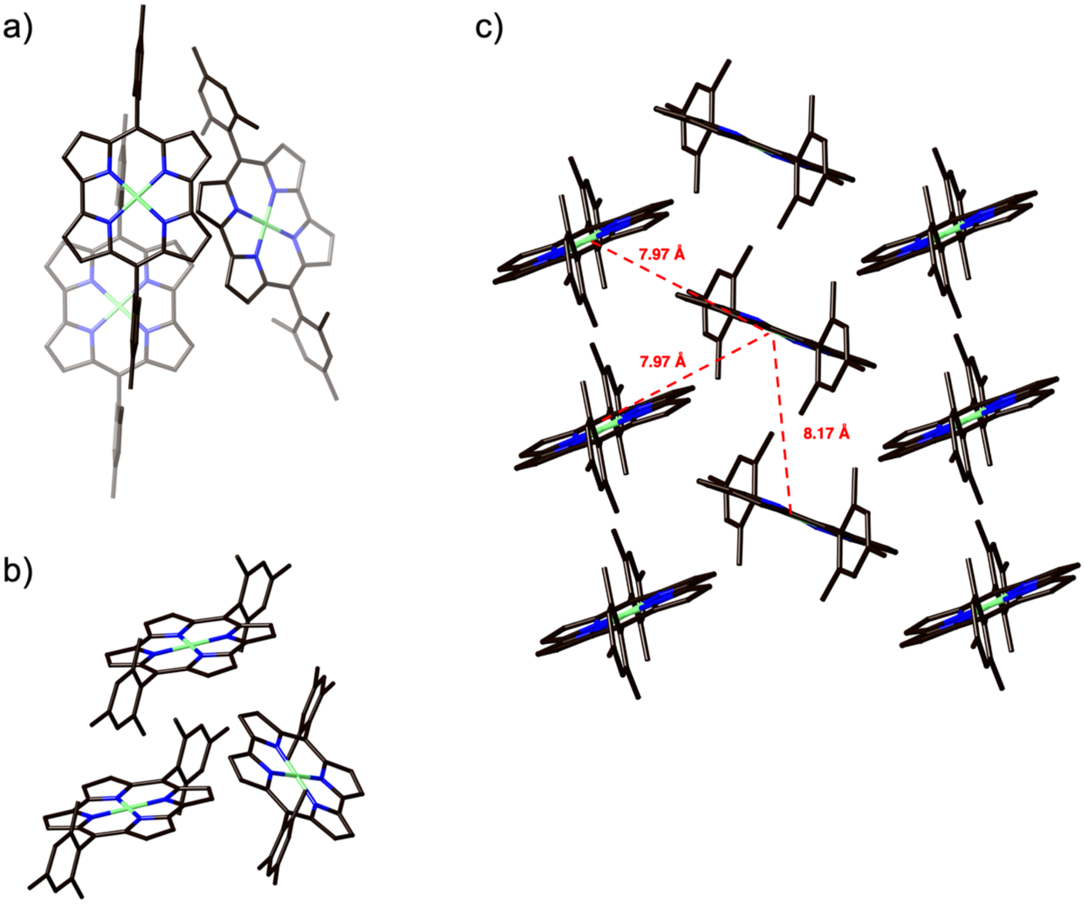

Fig. S25 Packing diagrams of **3** as well as their intermolecular distances. The intermolecular distance is defined as the distance between two nickel centers.

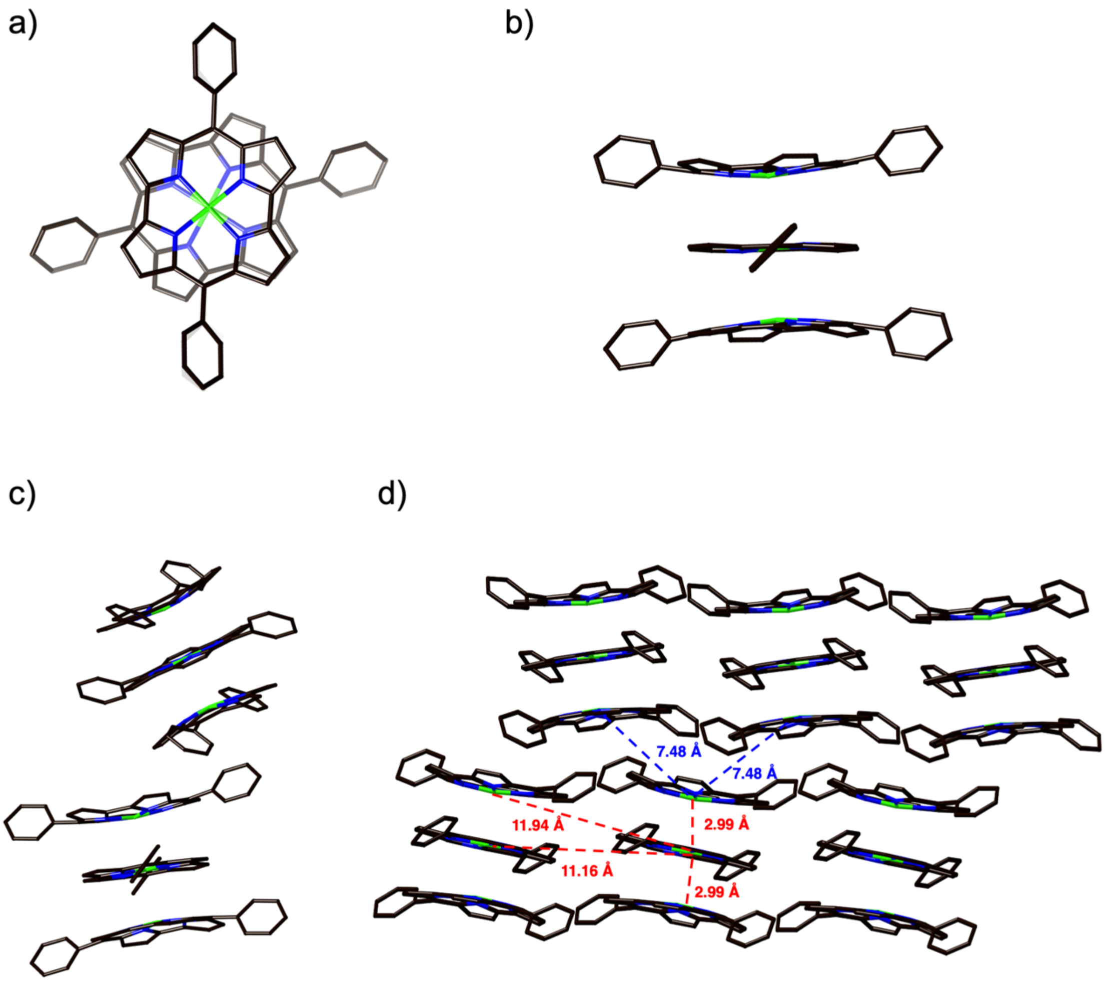

Fig. S26 Packing diagrams of **4** as well as their intermolecular distances. The intermolecular distance is defined as the distance between two nickel centers.

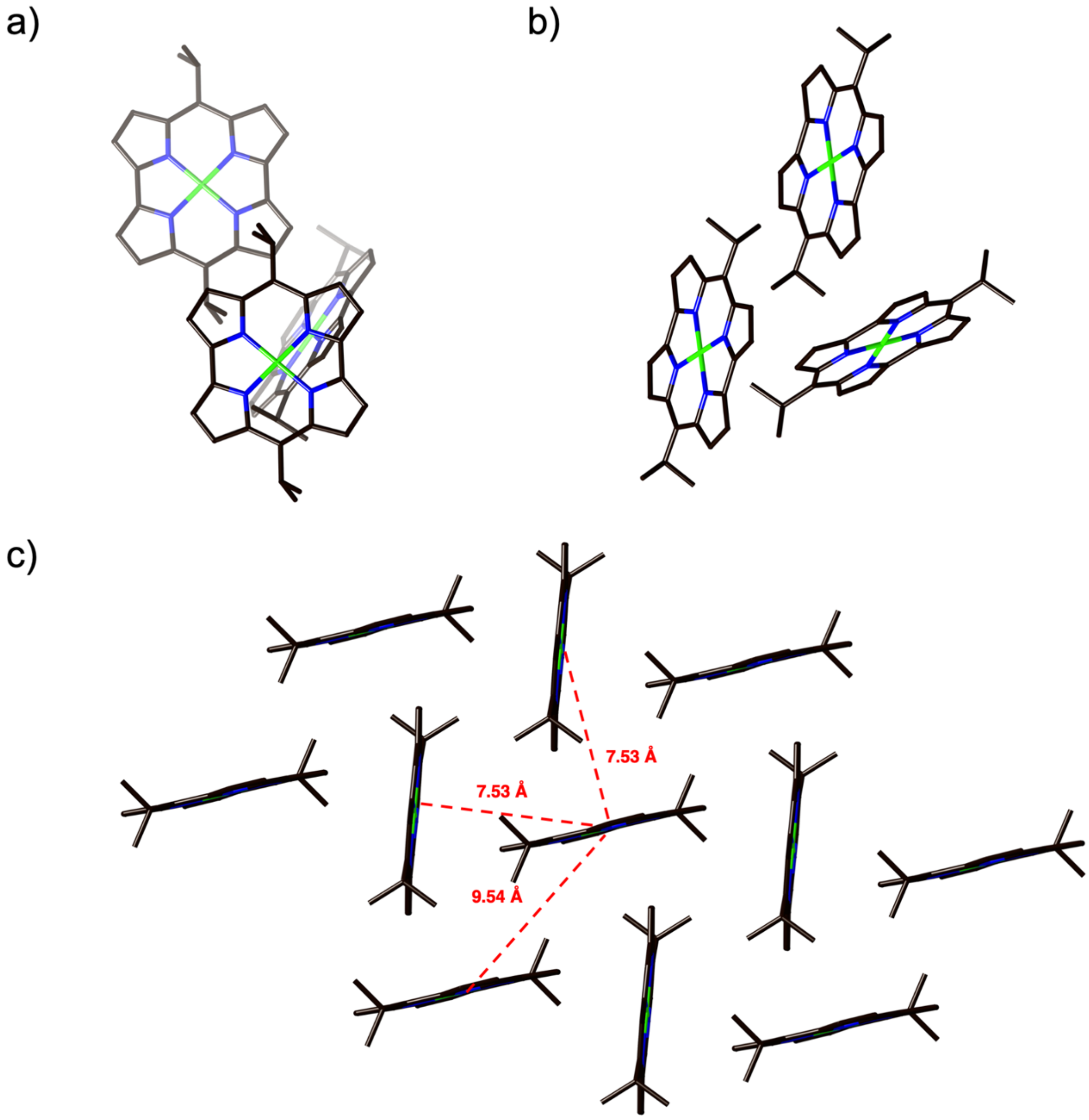

Fig. S27 Packing diagrams of **5** as well as their intermolecular distances. The intermolecular distance is defined as the distance between two nickel centers.

12. TRMC Measurements

Transient photoconductivity was measured by a FP-TRMC setup. A resonant cavity with $Q \sim 2500$ was used to obtain a high degree of sensitivity in the conductivity measurement. Proving microwave frequency and power were set at ~9.1 GHz and 3.0 mW, respectively, such that the electric field of the microwave was sufficiently small not to disturb the translational motion of charge carriers. The observed value of photoconductivity converted to the product of the quantum yield ϕ and the sum of charge-carrier mobilities $\Sigma\mu$ by $\phi\Sigma\mu = \Delta\sigma\ (eI_0F_{\mathrm{light}})^{-1}$, where e, I_0, F_{light} and $\Delta\sigma$ are the unit charge of a single electron, incident photon density of excitation laser (photons per m^2), a correction factor (m^{-1}) and a transient photoconductivity, respectively. The sample was set at the point of electric field maximum in a resonant cavity. FP-TRMC experiments were performed at room temperature, and under O_2 or Ar saturated conditions by continuous flowing > 10 min. The measurements of all the samples were performed for polycrystalline samples. These samples were fixed on a quartz substrate by poly(vinlyalcohol) binders.

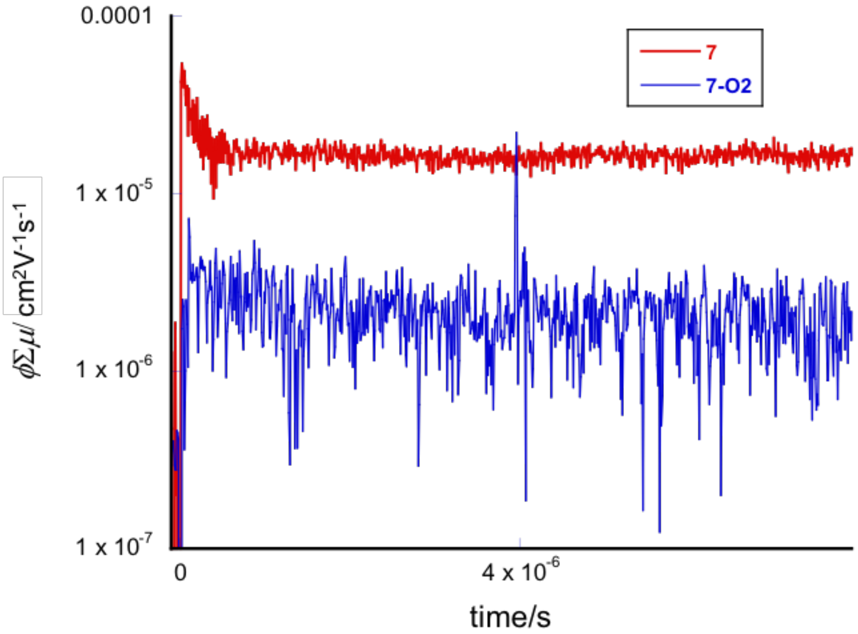

Fig. S28 Photoconductivity transients recorded in microcrystalline **7** under Ar (red) and O_2 (blue) saturated environment, respectively upon excitation at 355 nm, 0.2–1.3 × 10^{15} photons cm^{-2}, RT.

13. DFT Calculations

All calculations were conducted using the *Gaussian 09* program.[4] Initial geometry of **7** was obtained from its X-ray structure. The gas phase geometry was optimized with Becke's three-parameter hybrid exchange functional and the Lee–Yang–Parr correlation functional (B3LYP)[5] and a basis set consisting of SDD[6] for Ni and 6-31G(d) for the rest. The NICS calculations were conducted with the GIAO method at the B3LYP/6-31G(d)+SDD level.

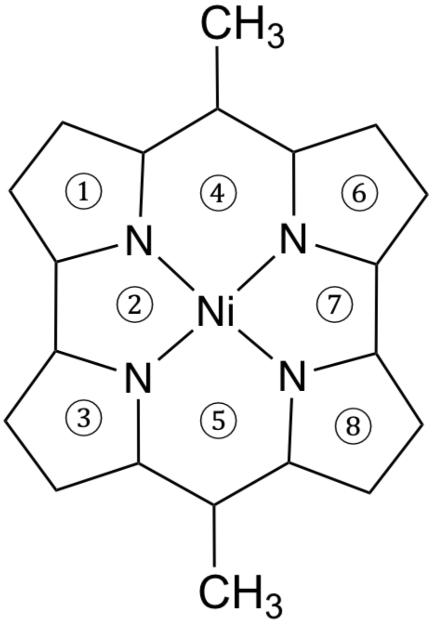

	NICS(0) [ppm] X-ray structure	NICS(0) [ppm] Optimerization structure	NICS(1) [ppm] Optimerization structure
①	4.85	3.66	2.75
②	40.93	35.41	31.20
③	5.04	3.66	2.79
④	40.26	35.58	29.80
⑤	40.29	35.58	29.92
⑥	5.08	3.66	2.75
⑦	41.01	35.41	31.21
⑧	4.85	3.66	2.79

Fig. S29 NICS values of **3**.

14. Calculation of Intermolecular Charge Transfer Integrals

The values of intermolecular charge transfer integrals were calculated with the corresponding dimer structures in the crystal packing of each Ni(II) norcorrole complex with the PW91/LANL2DZ level using CATNIP in conjunction with *Gaussian 16* package.[7],[8] The non-hybrid PW91[9] functional was used as the basis sets for transfer integral calculation, which has been known to give better estimates of transfer integral and reduce simultaneously calculation cost.[10] The values of charge transfer integrals of **3**, **4**, **5**, and **7** are shown with the schematic crystalline structure in Fig. S30.

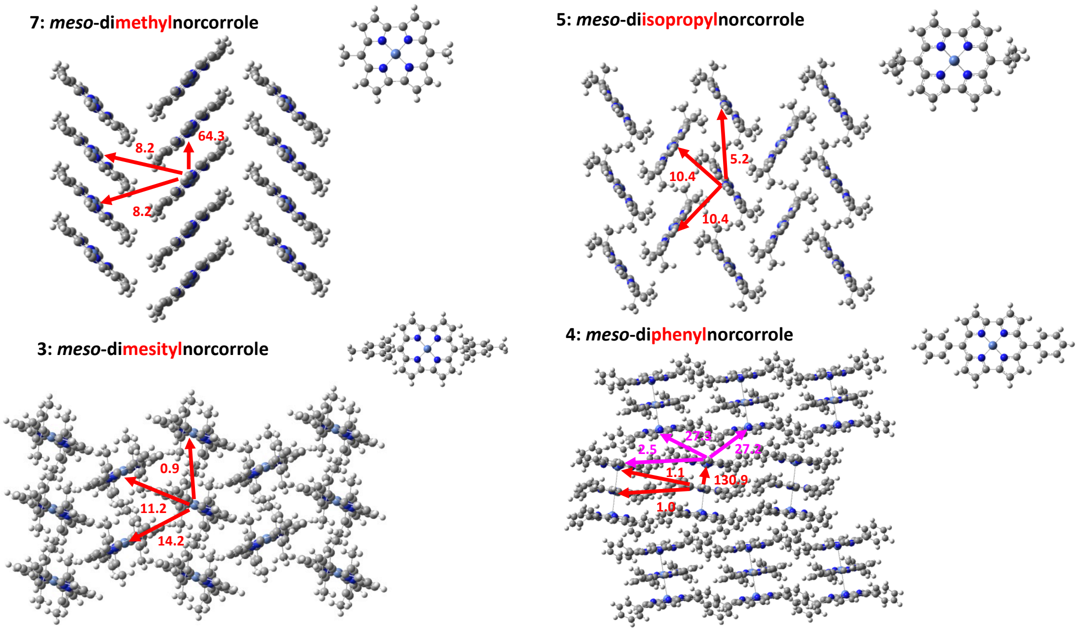

Fig. S30 Effective transfer integrals (meV) of LUMO calculated for nearest intralayer neighbors in the crystal structure of **3**, **4**, **5**, and **7**.

15. References

[1] Singhal, A.; Singh, S.; Chauhan, S. M. S. *Arkivoc* **2016**, *6*, 144.

[2] Nozawa, R.; Tanaka, H.; Cha, W.-Y.; Hong, Y.; Hisaki, I.; Shimizu, S.; Shin, J.-Y.; Kowalczyk, T.; Irle, S.; Kim, D.; Shinokubo, H. *Nat. Commun.* **2016**, *7*, 13620.

[3] (a) Ito, T.; Hayashi, Y.; Shimizu, S.; Shin, J.-Y.; Kobayashi, N.; Shinokubo, H. *Angew. Chem. Int. Ed.* **2012**, *51*, 8542; (b) Liu, S.-Y.; Tanaka, H.; Nozawa, R.; Fukui, N.; Shinokubo, H. *Chem. Eur. J.* **2019**, *25*, 7618; (c) Kido, H.; Shin, J.-Y.; Shinokubo, H. *Angew. Chem. Int. Ed.* **2013**, *52*, 13727.

[4] *Gaussian 09*, Revision D.01, Frisch, M. J.; Trucks, G. W.; Schlegel, H. B.; Scuseria, G. E.; Robb, M. A.; Cheeseman, J. R.; Scalmani, G.; Barone, V.; Mennucci, B.; Petersson, G. A.; Nakatsuji, H.; Caricato, M.; Li, X.; Hratchian, H. P.; Izmaylov, A. F.; Bloino, J.; Zheng, G.; Sonnenberg, J. L.; Hada, M.; Ehara, M.; Toyota, K.; Fukuda, R.; Hasegawa, J.; Ishida, M.; Nakajima, T.; Honda, Y.; Kitao, O.; Nakai, H.; Vreven, T.; Montgomery, Jr., J. A.; Peralta, J. E.; Ogliaro, F.; Bearpark, M.; Heyd, J. J.; Brothers, E.; Kudin, K. N.; Staroverov, V. N.; Kobayashi, R.; Normand, J.; Raghavachari, K.; Rendell, A.; Burant, J. C.; Iyengar, S. S.; Tomasi, J.; Cossi, M.; Rega, N.; Millam, J. M.; Klene, M.; Knox, J. E.; Cross, J. B.; Bakken, V.; Adamo, C.; Jaramillo, J.; Gomperts, R.; Stratmann, R. E.; Yazyev, O.; Austin, A. J.; Cammi, R.; Pomelli, C.; Ochterski, J. W.; Martin, R. L.; Morokuma, K.; Zakrzewski, V. G.; Voth, G. A.; Salvador, P.; Dannenberg, J. J.; Dapprich, S.; Daniels, A. D.; Farkas, Ö.; Foresman, J. B.; Ortiz, J. V.; Cioslowski, J.; Fox, D. J. Gaussian, Inc., Wallingford CT, **2009**.

[5] (a) Becke, A. D. *Phys. Rev. A* **1988**, *38*, 3098. (b) Lee, C.; Yang, W.; Parr, R. G. *Phys. Rev. B* **1988**, *37*, 785.

[6] Dolg, M.; Wedig, U.; Stoll, H.; Preuss, H. *J. Chem. Phys.* **1987**, *86*, 866.

[7] Brown, J. S. (2018). CATNIP (Version 1.9). [Software]. Available from https://github.com/JoshuaSBrown/QC_Tools.

[8] *Gaussian 16*, Revision A.03, M. J. Frisch, G. W. Trucks, H. B. Schlegel, G. E. Scuseria, M. A. Robb, J. R. Cheeseman, G. Scalmani, V. Barone, G. A. Petersson, H. Nakatsuji, X. Li, M. Caricato, A. V. Marenich, J. Bloino, B. G. Janesko, R. Gomperts, B. Mennucci, H. P. Hratchian, J. V. Ortiz, A. F. Izmaylov, J. L. Sonnenberg, D. Williams-Young, F. Ding, F. Lipparini, F. Egidi, J. Goings, B. Peng, A. Petderson, D. Ranasinghe, V. G. Zakrzewski, J. Gao, N. Rega, G. Zheng, W. Liang, M. Hada, M. Ehara, K. Toyota, R. Fukuda, J. Hasegawa, M. Ishida, T. Nakajima, Y. Honda, O. Kitao, H. Nakai, T. Vreven, K. Throssell, J. A. Montgomery, Jr., J. E. Peralta, F. Ogliaro, M. J. Bearpark, J. J. Heyd, E. N. Brothers,

K. N. Kudin, V. N. Staroverov, T. A. Keith, R. Kobayashi, J. Normand, K. Raghavachari, A. P. Rendell, J. C. Burant, S. S. Iyengar, J. Tomasi, M. Cossi, J. M. Millam, M. Klene, C. Adamo, R. Cammi, J. W. Ochterski, R. L. Martin, K. Morokuma, O. Farkas, J. B. Foresman, and D. J. Fox, Gaussian, Inc., Wallingford CT, **2016**

[9] J. P. Perdew, in Electronic Structure of Solids, ed. P. Ziesche and H. Eschrig, Akademie Verlag, Berlin, **1991**, p. 11.

[10] J. Huang, M. Kertesz, *J. Chem. Phys.*, **2005**, *122*, 234707.